(Qualifying Exam)

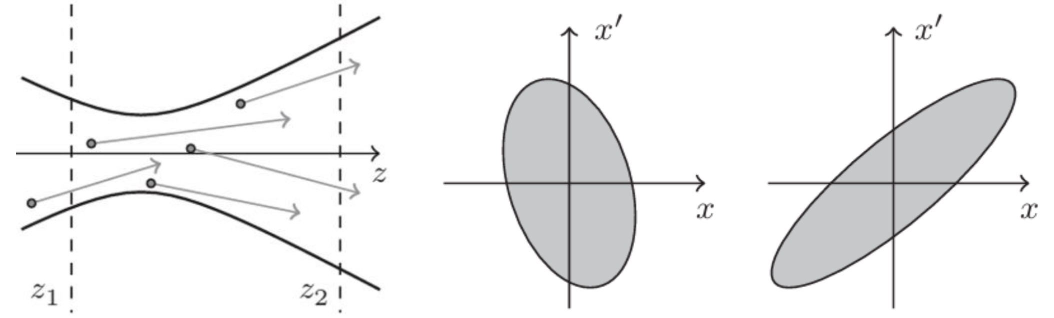

Kim et al, “Synchrotron radiation and free electron lasers”, Cambridge University Press (2017)

Exploring the quasi-6D structure of laser-wakefield-accelerated electron bunches with coherent optical transition radiation

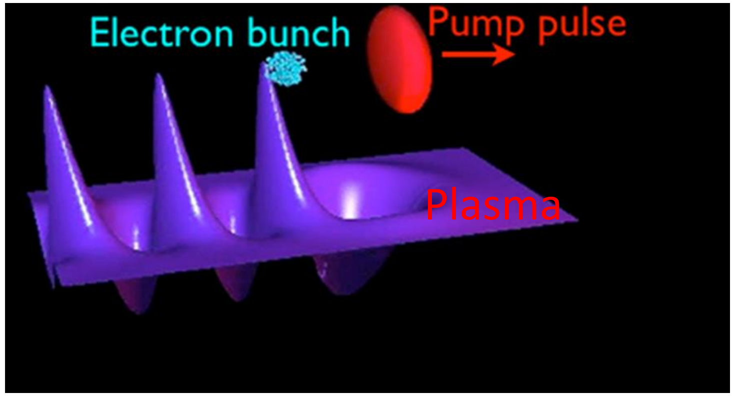

Malka, *Phys. Plasma* **19**, 055501 (2012)

Ze Ouyang

Supervisor: Michael Downer

6th Nov, 2024

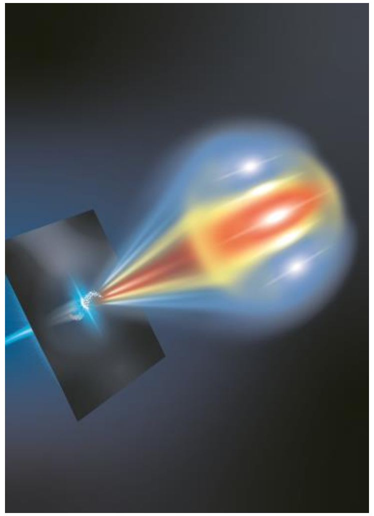
LaBerge, AAC 2024

Outline

1. Introduction to LWFA and its diagnostics
2. COTR(I) and quasi-6D structure of e- bunches
3. Future directions, experimental work & conclusion

Useful abbreviations:

- LWFA: Laser-driven WakeField Accelerator
- TR: Transition Radiation
- COTR: Coherent Optical Transition Radiation
- COTRI: Coherent Optical Transition Radiation Interferometry

Introduction: Laser-driven WakeField Accelerator

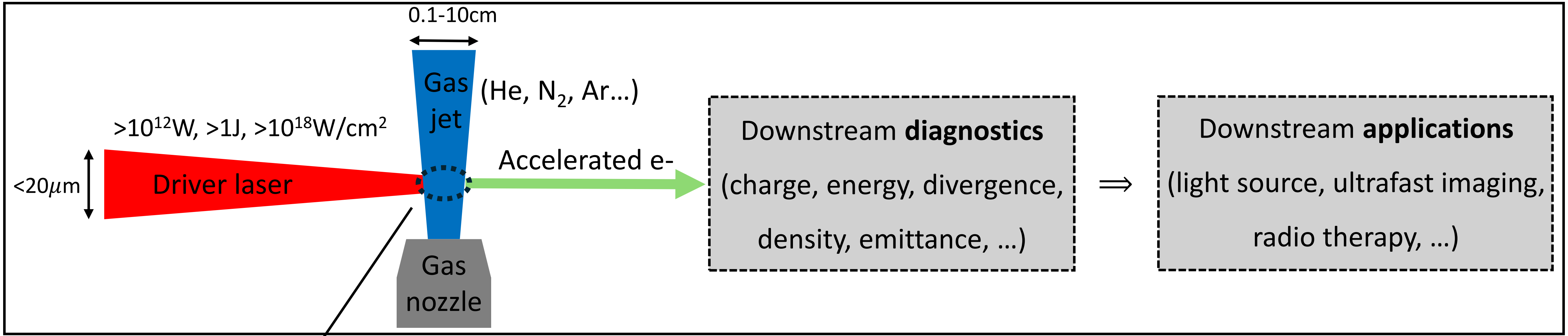

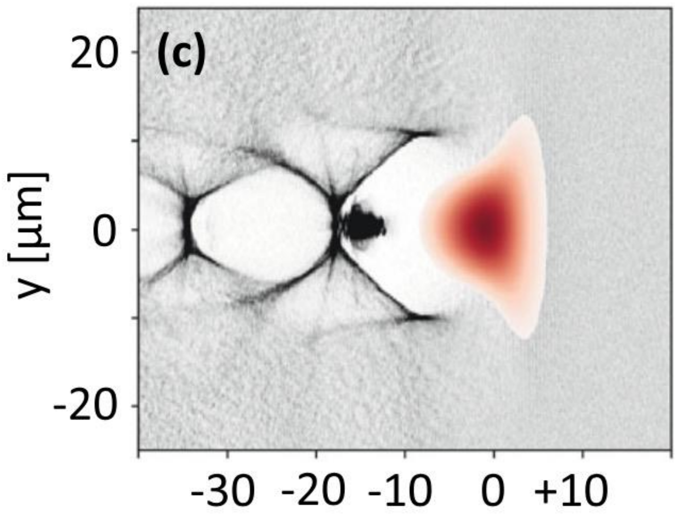

Downer et al, *Rev. Mod. Phys.* **90**, 035002 (2018)

LWFA ∈ plasma-based accelerator[1]

	Plasma-	Conventional (SLAC)
E	100GV/m	100MV/m
Footprint	~m	~km
Max Energy	10GeV[2]	50GeV
Cost	~few $millions	114 $millions in 1960s

Plasma-	Conventional
<100pC	~nC
~μm	~10μm
<10fs	~100fs
~mrad	~μrad

We need new diagnostics.

1 Tajima et al, *Phys. Rev. Lett.* **43**, 4 (1979)
2 Aniculaesei et al, *MRE* **9**, 014001 (2024)

Introduction: LWFA diagnostics

e- beams from LWFA can be:

- transversely small: 0.1 μm<σ_r<1 μm
- longitudinally short: 0.03 μm<σ_z<3 μm (0.1 fs<σ_z/c<10 fs)
- highly divergent: 1 mrad<σ_r'<10 mrad

  $\Rightarrow$ transverse normalized emittance: 0.1 mm mrad<ε_n<1 mm mrad
- **microbunched**: e- grouped into subtle structure within sub- μm range (**Today's diagnostics frontier**)
- bunch charge, energy spread, repetition rate, efficiency et al.

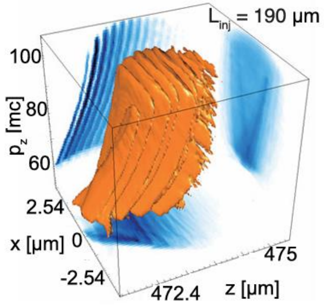

"Microbunched e- beam in LWFA"

Xu et al, *Phys. Rev. Lett* **117**, 034801 (2016)

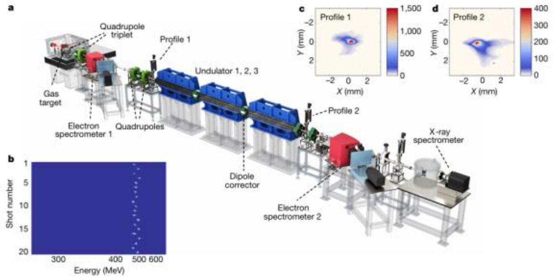

"Microbunched e- beam in LWFA-based Free Electron Laser"

Wang et al. *Nature* **595**, 516-520 (2021)

Emittance[1]: $\varepsilon_x \equiv \sqrt{\langle x^2\rangle\langle x'^2\rangle - \langle xx'\rangle^2}$.

Normalized emittance: $\varepsilon_{x,n} = \beta_z\gamma\,\varepsilon_x \approx \gamma\,\varepsilon_x$.

1. $\propto$ area of e- occupied in 6D phase space
2. Conserved in ideal beam transportation

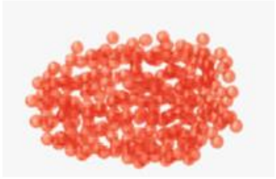

non-mb

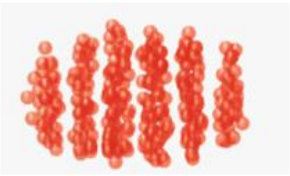

mb

Eur. Phys. J. Spec. Top. 233: 1-208 (2024)

- Microbunched e- structure (**only**) by COTR (3D)
- Transverse divergence by COTRI (2D)
- z-dependent transverse divergence by COTRI and physical constraints (quasi-1D)

COTR $\Rightarrow$**quasi-6D structure**

1 Corde et al, *Rev. Mod. Phys.* **85**, 000001 (2013)

Outline

1 Introduction to LWFA and its diagnostics

2 COTR(I) and quasi-6D structure of e- bunches

3 Future directions, experimental work & conclusion

Useful abbreviations:

- LWFA: Laser-driven WakeField Accelerator
- TR: Transition Radiation
- COTR: Coherent Optical Transition Radiation
- COTRI: Coherent Optical Transition Radiation Interferometry

Transition Radiation (single e-)

TR is emitted when charged particle passes from one medium into another with different index of refractive.

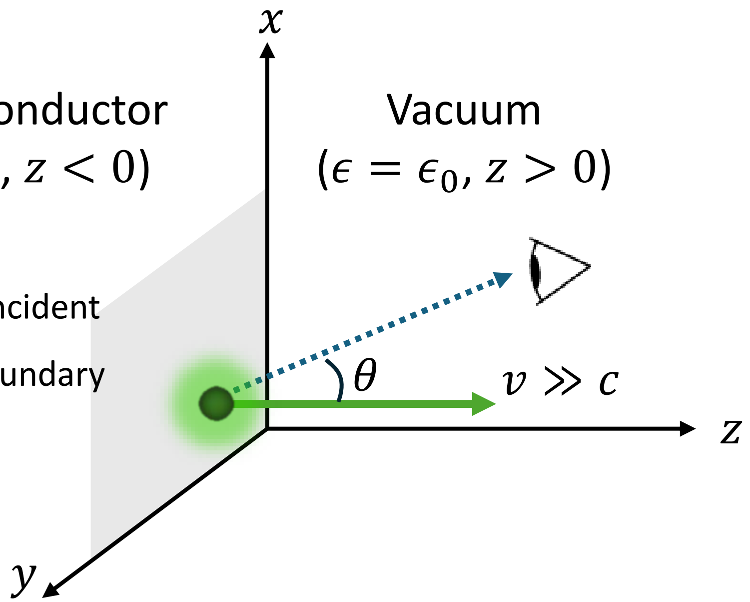

- Normally incident
- Steplike boundary

Single e- TR energy[1] in far field :

$$\frac{\mathrm{d}^2 W_1}{\mathrm{d}\omega \mathrm{d}\Omega} = \frac{e^2}{4\pi^3 \epsilon_0 c} \frac{\beta^2 \sin^2\theta}{(1 - \beta^2 \cos^2\theta)^2}$$

1. target radiating & radially polarized
2. broadband (low- and high- ω cutoff: 0.2μm-10μm)
3. narrow cone (peaked at $\theta \sim \frac{1}{\gamma}$) & weakly γ-dependent ($\gamma \gg 1$)

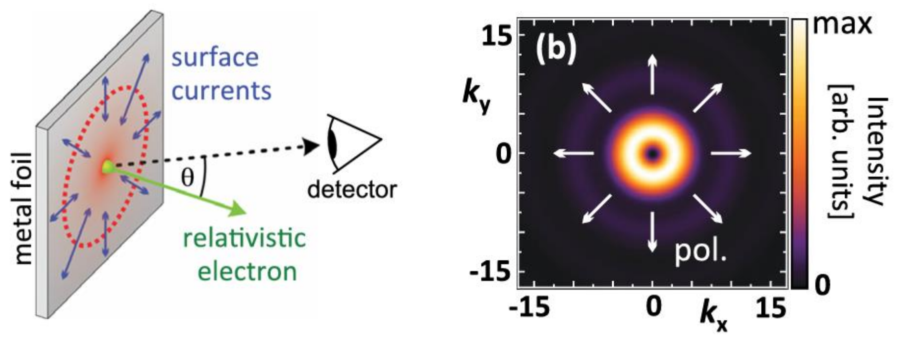

Rev. Mod. Phys. **90**, 035002 (2018)

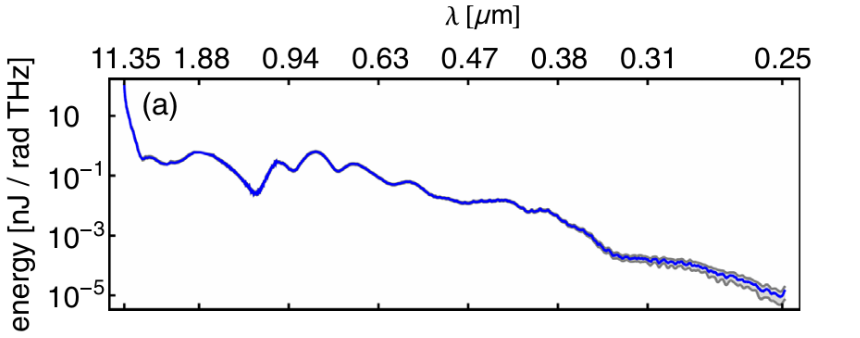

Phys. Rev. Accel. Beams **25**, 012801 (2022)

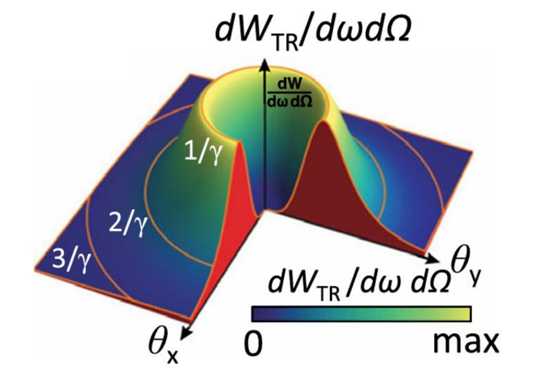

Rev. Mod. Phys. **90**, 035002 (2018)

1 Schroeder et al, *Phys. Rev. E* **69**, 016501 (2004)

Transition Radiation (e- bunch)

In the case of multiple e-:

$$\frac{d^2 W_N}{d\omega d\Omega} = [\underline{N} + \underline{N(N-1)} \cdot |F(\omega,\theta)|^2] \cdot \frac{d^2 W_1}{d\omega d\Omega}$$

E field

- Out-of-phase emission $\propto N$ (incoherent)
- In-phase emission $\propto N^2$ (coherent)

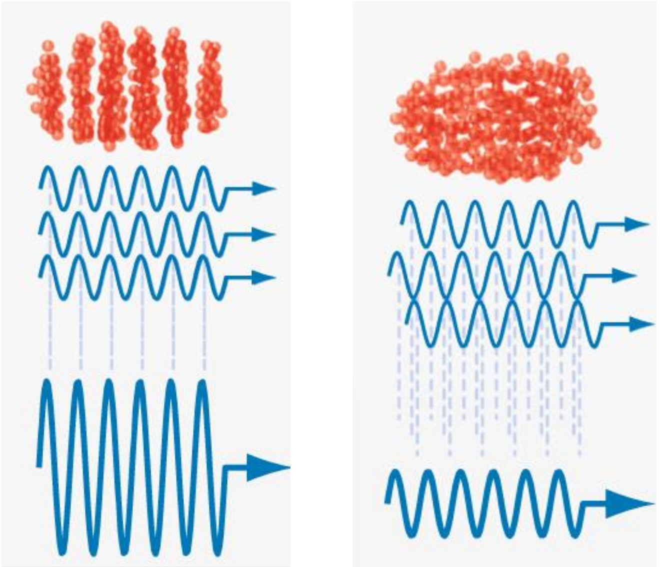

Eur. Phys. J. Spec. Top. 233: 1-208 (2024)

where $F(\omega,\theta)$ is the form factor (level of coherence)

$$F(\omega,\theta) = \int \rho(\boldsymbol{r}) e^{i\boldsymbol{kr}} d\boldsymbol{r}$$

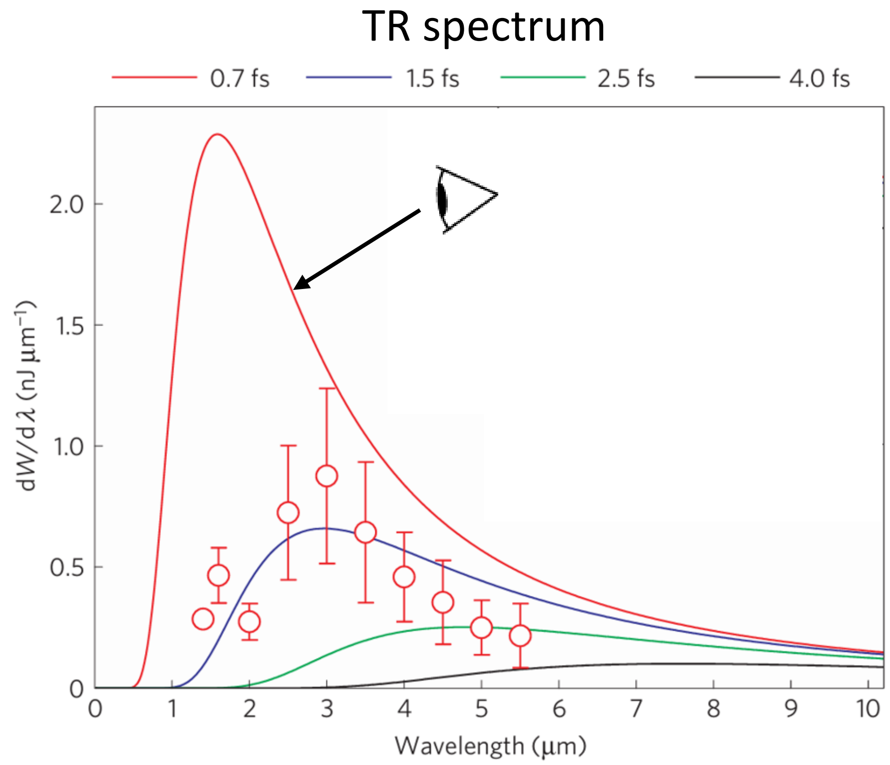

Lundh et al, *Nat. Phys.* **7**, 219-222 (2011)

- $\lambda > \sigma_z$: incoherent
- $\lambda < \sigma_z$: coherent
- microbunched e- beam: λ is coherent down to **optical range** (COTR)⇒structure info

Transition Radiation Imaging (single e- near field)

COTR is detected in the near field

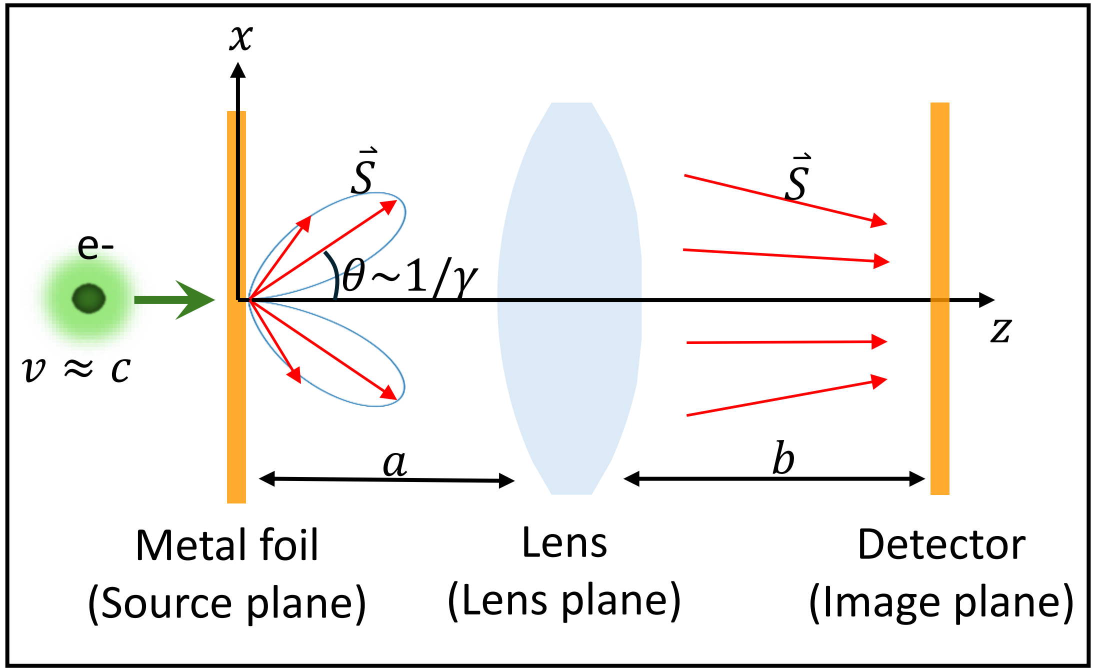

Source plane[1,2]:

$$E_{x,y}^{s}(x_s, y_s, \omega) = \frac{e\omega}{\pi v^2 \gamma} \frac{x_s, y_s}{\sqrt{x_s^2 + y_s^2}} K_1\left(\frac{\omega}{v\gamma}\sqrt{x_s^2 + y_s^2}\right)$$

scalar diffraction theory

Lens plane:

$$E_{x,y}^{li}(x_s, y_s, \omega) = -\frac{ie^{ika}}{\lambda a} e^{ik\frac{x_l^2+y_l^2}{2a}} \int \mathrm{d}x_s \mathrm{d}y_s\, E_{x,y}^{s} e^{-ik\frac{x_l x_s + y_l y_s}{2a}} e^{ik\frac{x_s^2+y_s^2}{2a}}$$

$$E_{x,y}^{lo}(x_s, y_s, \omega) = E_{x,y}^{li}(x_s, y_s, \omega) e^{-ik\frac{x_l^2+y_l^2}{2f}}$$

scalar diffraction theory

Image plane:

$$E_{x,y}^{i}(x_s, y_s, \omega) = -\frac{ie^{ikb}}{\lambda b} e^{ik\frac{x_i^2+y_i^2}{2b}} \int \mathrm{d}x_l \mathrm{d}y_l\, E_{x,y}^{lo} e^{-ik\frac{x_l x_i + y_l y_i}{2b}} e^{ik\frac{x_i^2+y_i^2}{2b}}$$

$$\Rightarrow \boldsymbol{E}(x_i, y_i) = \frac{2e}{\lambda v M} f(\theta_m, \gamma, \zeta) \boldsymbol{e_r}$$ Field Point Spread Function(FPSF)

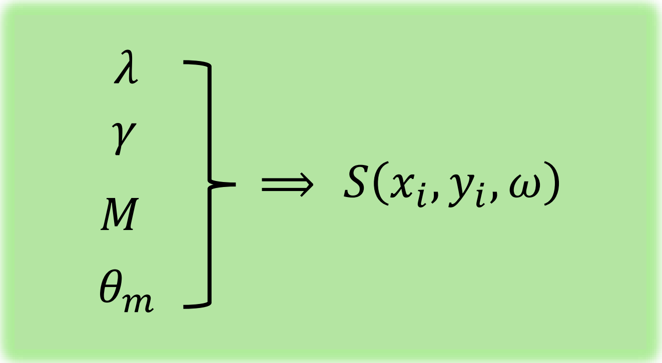

The energy flux per unit frequency interval is

$$S(x_i, y_i, \omega) = \frac{c}{4\pi^2}(|\boldsymbol{E}(x_i, y_i)|^2) = \frac{\mathrm{d}^3 W_1}{\mathrm{d}\omega \mathrm{d}x_i \mathrm{d}y_i}$$ Point Spread Function(PSF)

1 Castellano et al. *Phys. Rev. Accel. Beams* **1**, 062801 (1998)
2 Xiang et al. *Nucl. Instrum. Meth. A* **570**, 3 (2007)

Transition Radiation Imaging (single e- near field)

λ=500nm, M=1, γ=391(200MeV), and θ_m=0.1

PSF∝($|FPSF\_x|^2$+$|FPSF\_y|^2$)

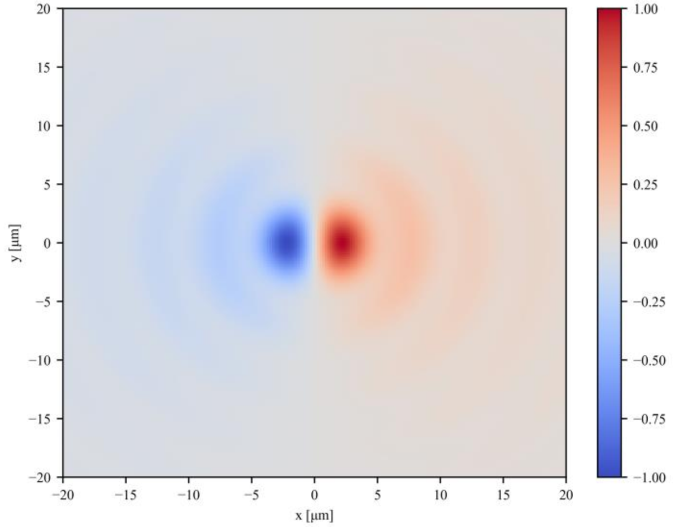

FPSF polarized in x-axis

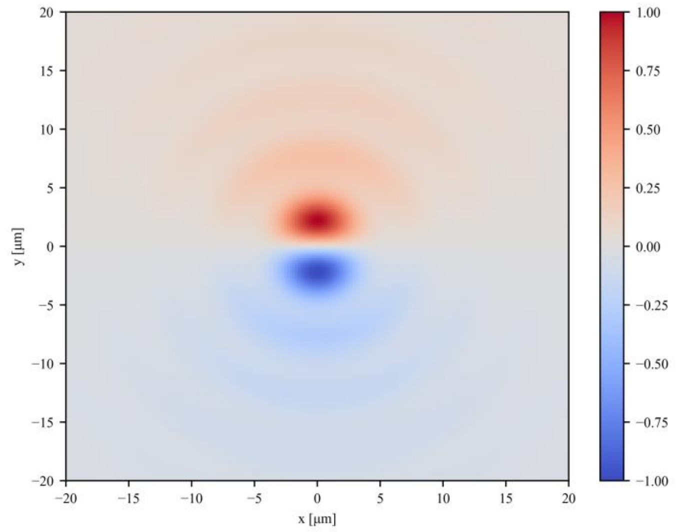

FPSF polarized in y-axis

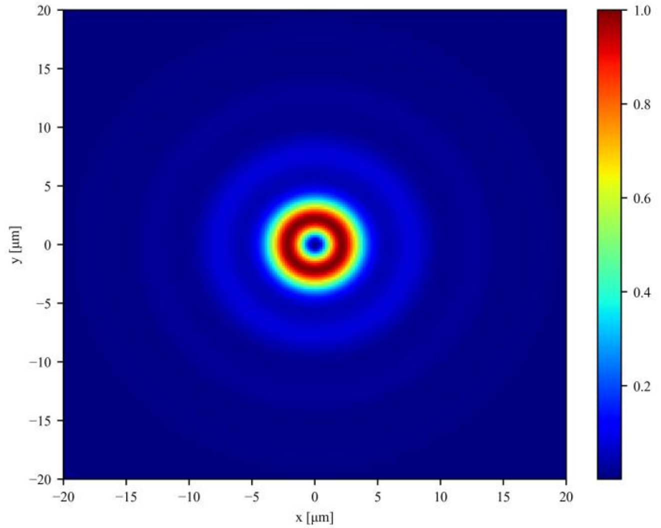

PSF

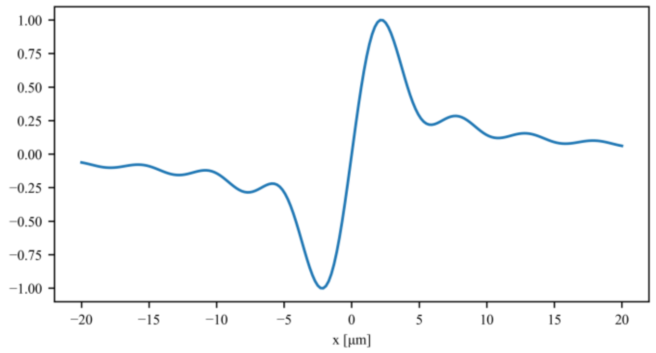

Lineout of FPSF_x at y=0

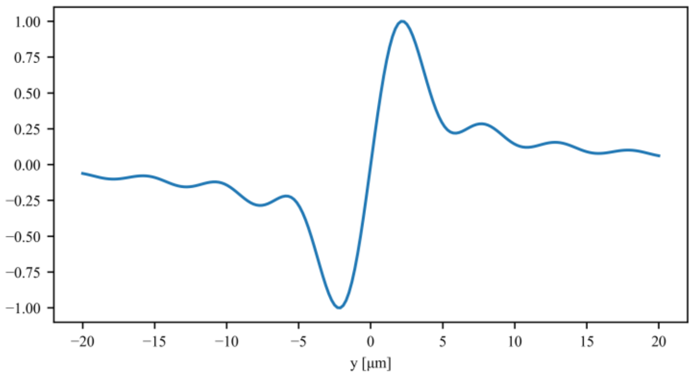

Lineout of FPSF_y at x=0

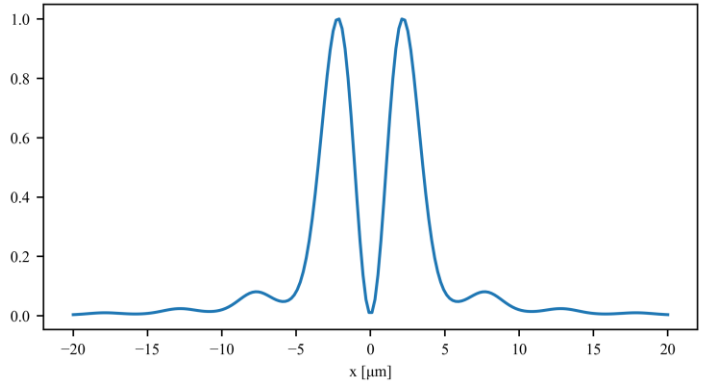

Lineout of PSF at y=0

Transition Radiation Imaging (e- bunch near field)

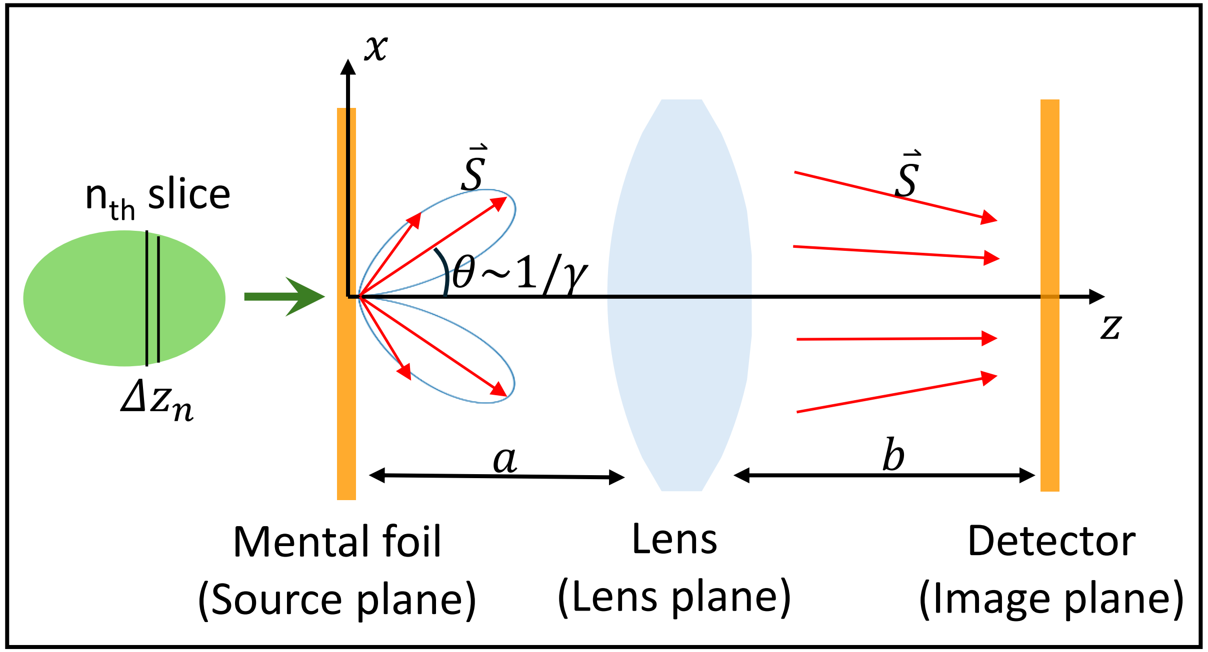

Electron number density $\rho(x_s, y_s, z_s)$

$$\boldsymbol{E}^{(n)}(x_i, y_i) = \Delta z_n \iint \mathrm{d}x_s \mathrm{d}y_s \, \rho(x_s, y_s, z_n) \mathrm{FPSF}(x_i - x_s, y_i - y_s)$$

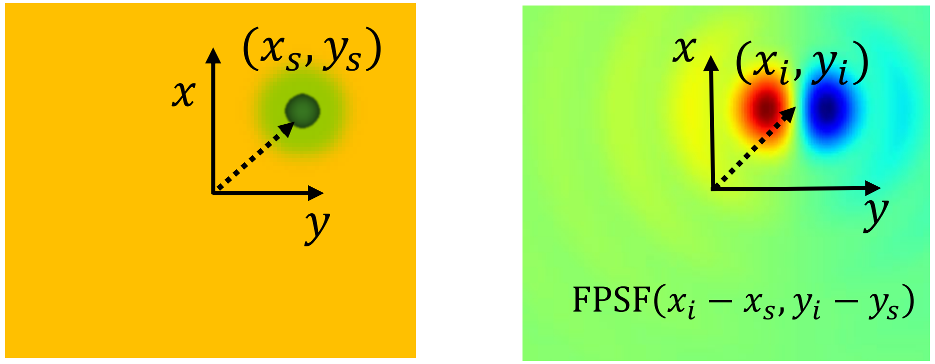

FPSF translation

Each slice has a phase delay[1] e^{ikz_n}

Total $\boldsymbol{E}$ field is

$$\boldsymbol{E}_{\mathbf{tot}}(x_i, y_i) = \iiint \mathrm{d}x_s \mathrm{d}y_s dz_s \cdot \rho(x_s, y_s, z_s) \cdot e^{ikz} \cdot \mathrm{FPSF}(x_i - x_s, y_i - y_s)$$

Total energy flux per unit frequency interval is

$$S_{\mathrm{tot}}(x_i, y_i, \omega) = \frac{c}{4\pi^2}(|\boldsymbol{E}_{\mathbf{tot}}(x_i, y_i)|^2) = \frac{\mathrm{d}^3 W_1}{\mathrm{d}\omega \mathrm{d}x_i \mathrm{d}y_i}$$

$$\left.\begin{matrix} \lambda \\ \gamma \\ M \\ \theta_m \\ \rho \end{matrix}\right\} \Longrightarrow S_{\mathrm{tot}}(x_i, y_i, \omega)$$

S contains info of ρ

1 Lin et al. *Phys. Rev. Lett.* **108**, 094801 (2012)

Revealing the $\rho(x_s, y_s, z_s)$ by COTR: an inverse problem

Forward process: $\rho(x_s, y_s, z_s) \Longrightarrow S(x_i, y_i)$

$$\left.\begin{array}{c}\lambda\\ \gamma\\ M\\ \theta_m\\ \rho\end{array}\right\} \Longrightarrow S_{\text{tot}}(x_i, y_i, \omega)$$

Backward process: $S(x_i, y_i) \Longrightarrow \rho(x_s, y_s, z_s)$

$$\left.\begin{array}{c}\lambda\\ \gamma\\ M\\ \theta_m\\ S_{\text{tot}}(x_i, y_i, \omega)\end{array}\right\} \Longrightarrow \rho$$

Without loss of generality, consider S as what is measured.

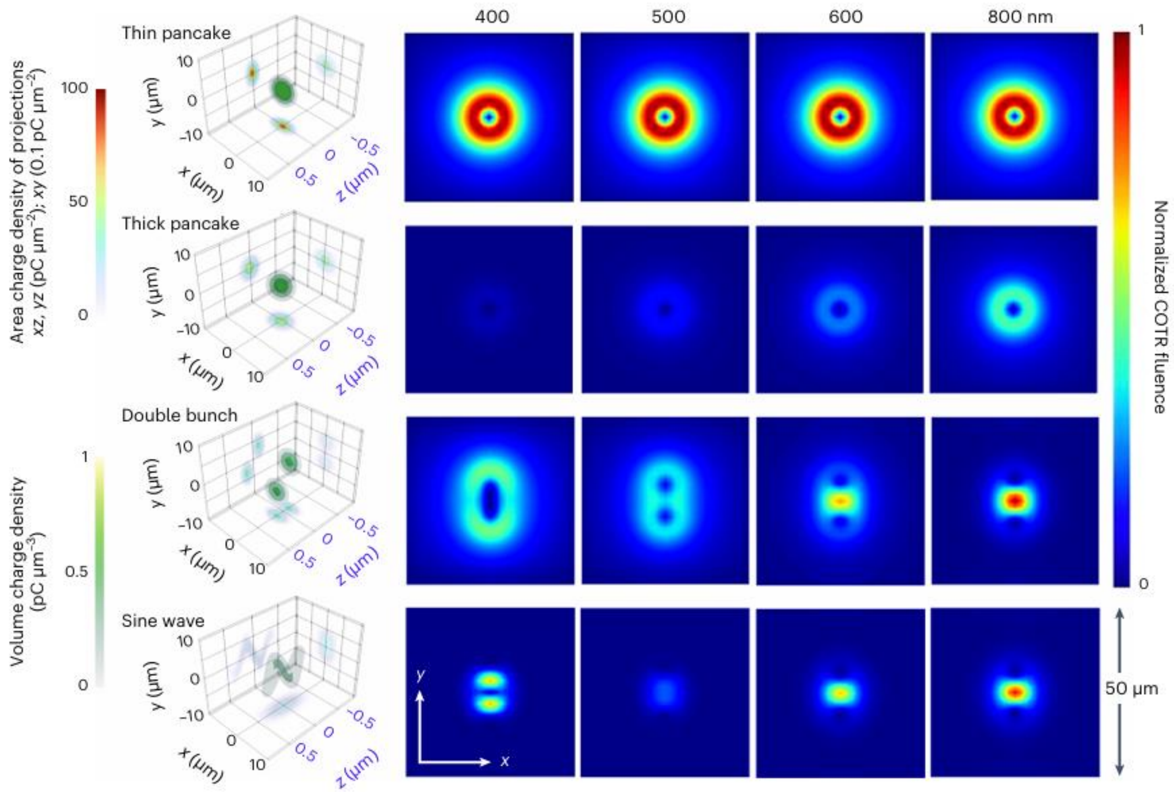

σ_z=300nm

σ_z=400nm

σ_z=300nm
L_z=400nm

T=800nm

LaBerge et al, *Nat. Photon.* **18** 952-959 (2024)

An inverse problem

Revealing the $\rho(x_s, y_s, z_s)$ by COTR: workflow

$$\rho(x_s, y_s, z_s) = \sum_{j=1}^{N} N_{e_j} \frac{1}{\sqrt{2\pi}\sigma_{x_j}} \exp\left(-\frac{\left(x-\mu_{x_j}\right)^2}{2\sigma_{x_j}^2}\right) \frac{1}{\sqrt{2\pi}\sigma_{y_j}} \exp\left(-\frac{\left(y-\mu_{y_j}\right)^2}{2\sigma_{y_j}^2}\right) \frac{1}{\sqrt{2\pi}\sigma_{z_j}} \exp\left(-\frac{\left(z-\mu_{z_j}\right)^2}{2\sigma_{z_j}^2}\right)$$

Suppose $\rho(x_e, y_e, z_e)$ is a parameterized function, i.e. sum of Gauss functions.

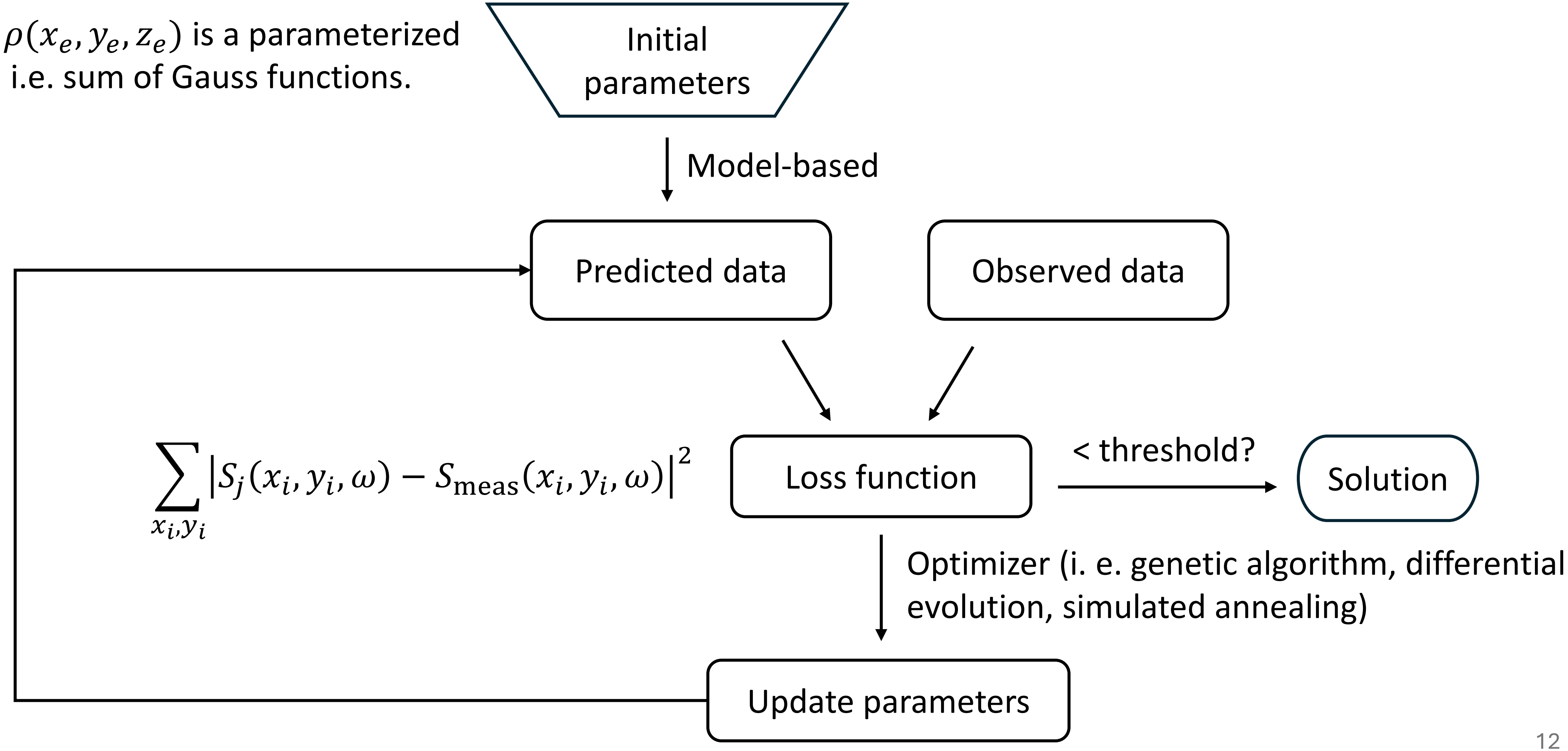

Revealing the $\rho(x_s, y_s, z_s)$ by COTR: Latest results

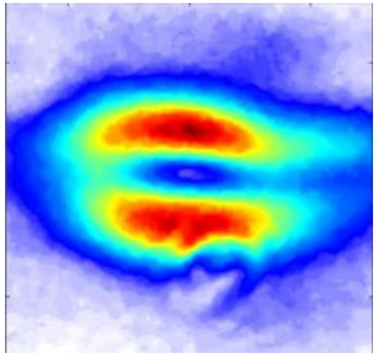

S_{meas} at 550nm

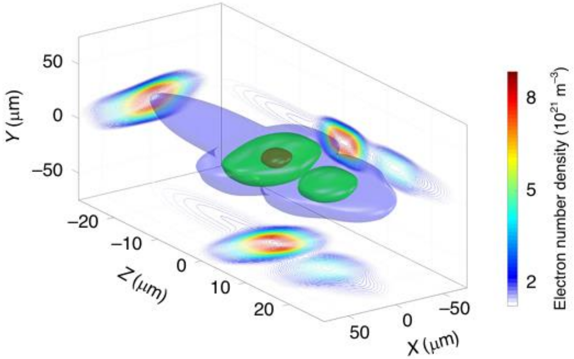

Huang et al. *Light: sci.appl* **13**, 1 (2024)

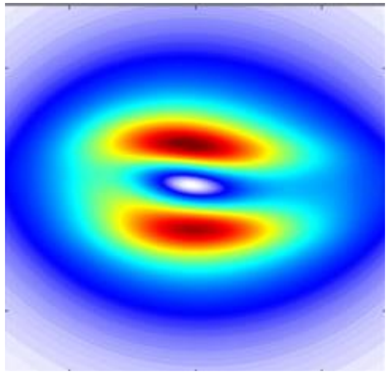

S_{rcn} at 550nm

Genetic algorithm

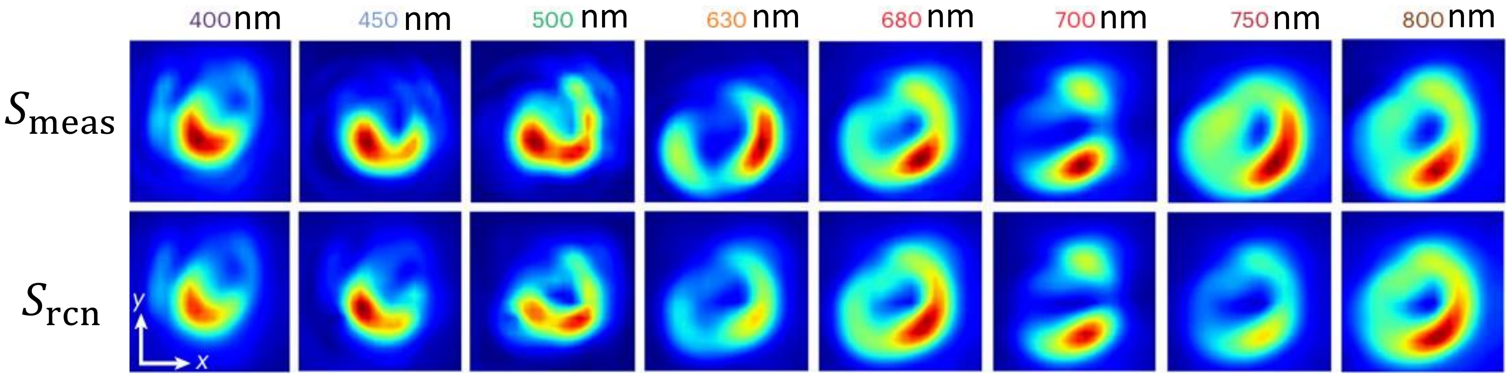

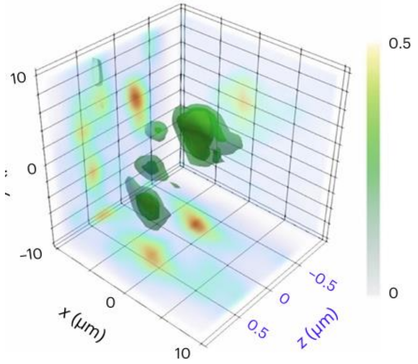

LaBerge et al, *Nat. Photon.* **18** 952-959 (2024)

Differential evolution

Revealing the $\rho(x_s, y_s, z_s)$ by COTR: uniqueness

Phase info lost in the forward process $\Longrightarrow$ reconstruction is not unique

How to compress the volume of solution space $\Longrightarrow$ **Knowing longitudinal profile in advance**!

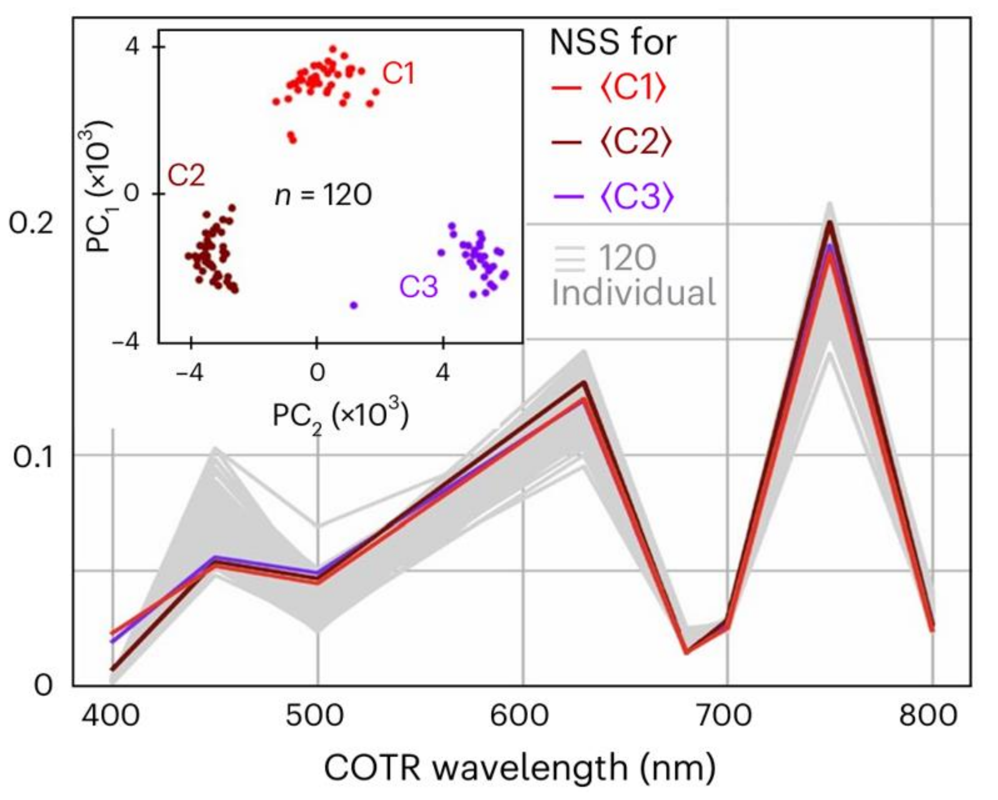

LaBerge et al, *Nat. Photon.* **18** 952-959 (2024)

Knowledge of e- beam longitudinal is **injection-regime-dependent**:

- Down ramp injection: e- spectrum
- Self-truncated ionization injection: PIC simulation
- Self injection: not accessible

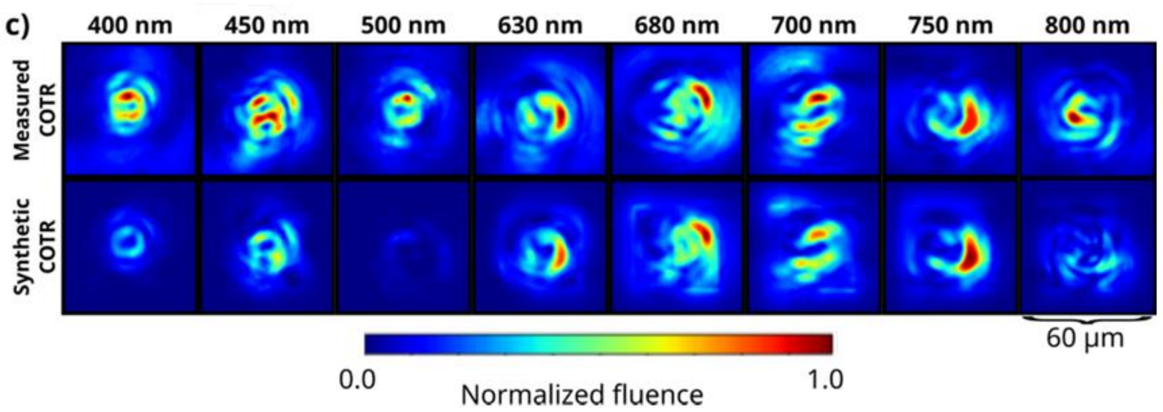

LaBerge et al, *Nat. Photon.* **18** 952-959 (2024)

Other architectures to solve such an inverse question?

Revealing the $\rho(x_s, y_s, z_s)$ by COTR: ML-workflow

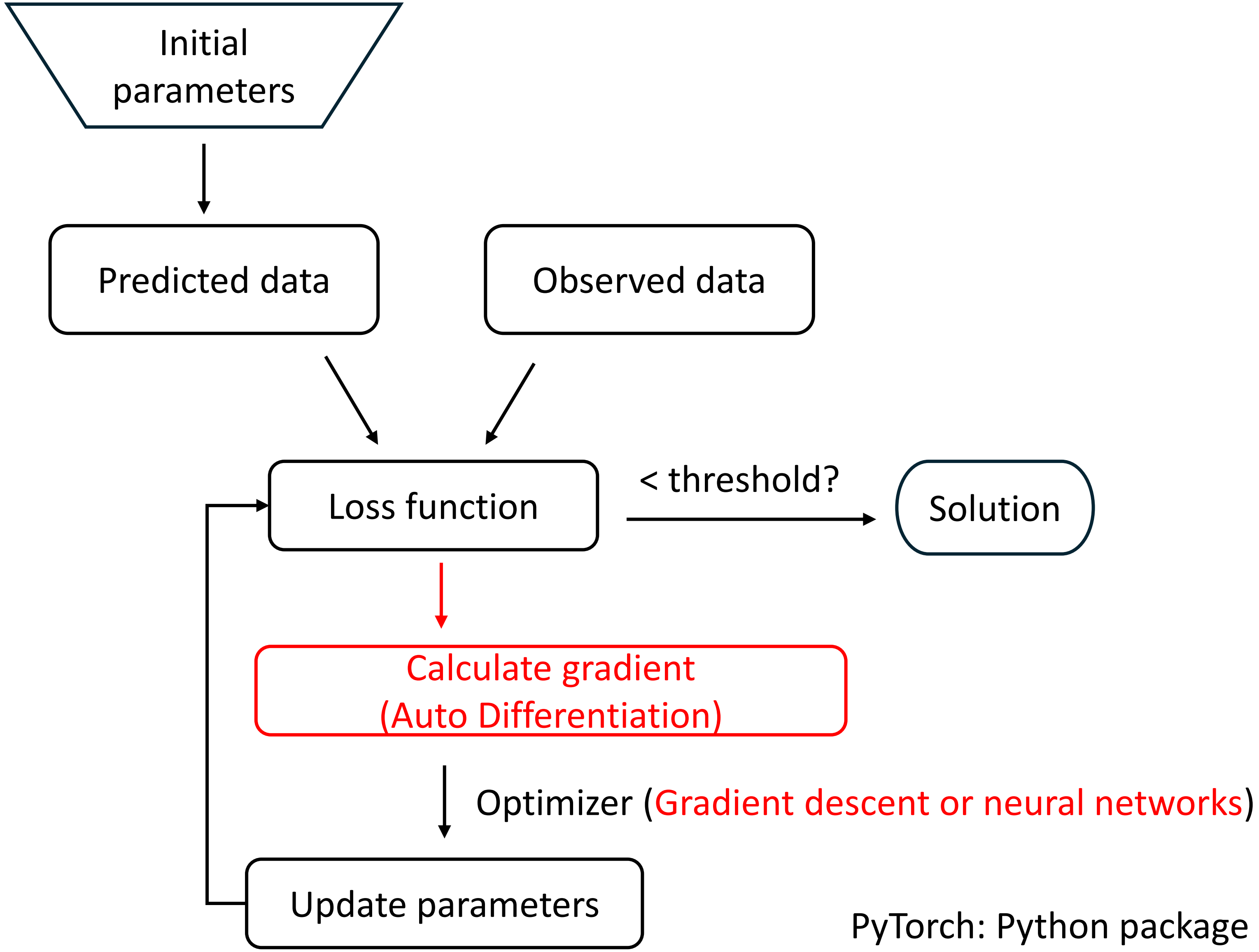

$$z = \sin(x_1 + x_2) + x_2^2 x_3$$

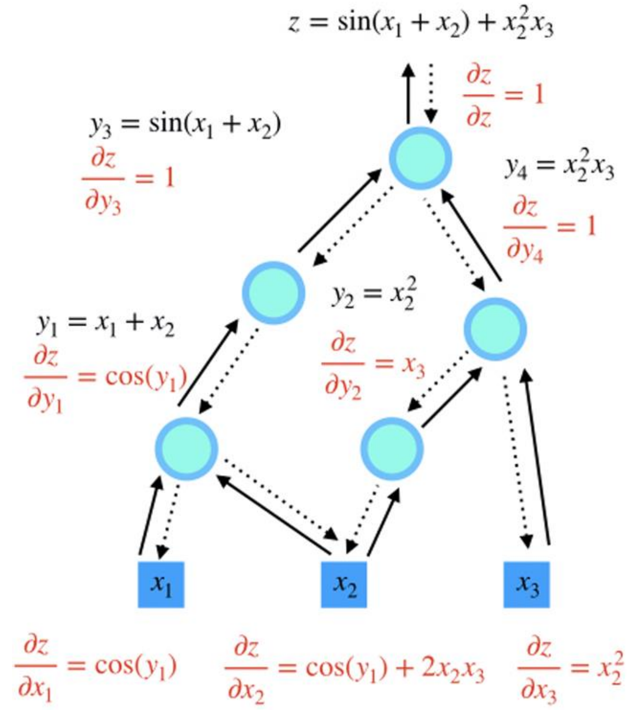

Computation Graph

https://github.com/kailaix/ADCME.jl

PyTorch: Python package for
- GPU computation
- Auto Differentiation (AD)
- Machine Learning (ML)

Revealing the $\rho(x_s, y_s, z_s)$ by COTR: Gradient descent

400nm 450nm 500nm 630nm 680nm 700nm 750nm 800nm

"S_{meas}"
26 Gauss

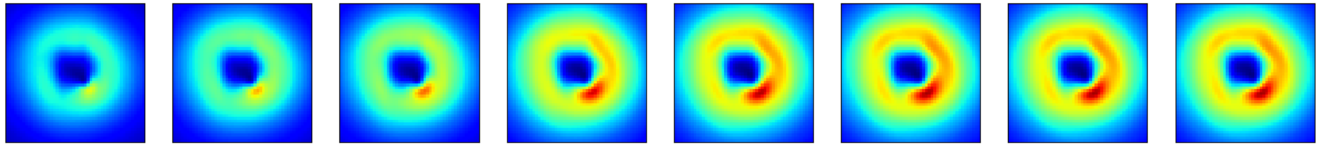

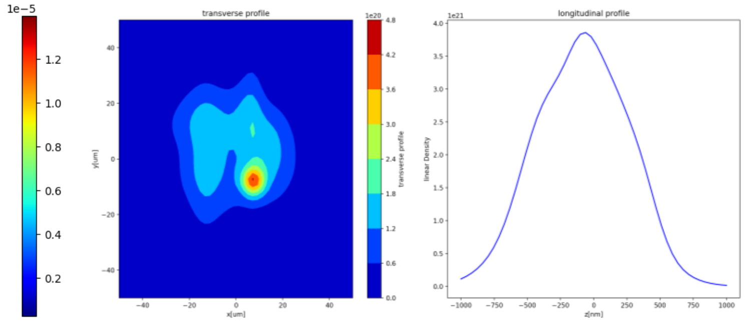

S_{seed}
50 Gauss

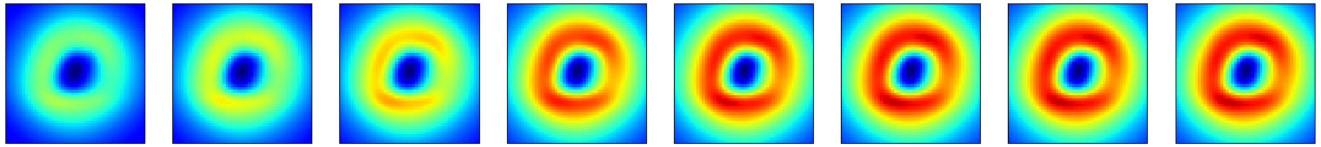

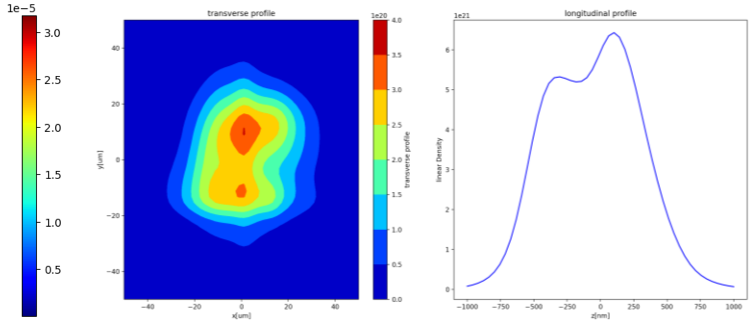

Loss function: $\sum_{x_i, y_i} \left| S_j(x_i, y_i, \omega) - S_{\mathrm{meas}}(x_i, y_i, \omega) \right|^2$

iterate

S_{rcn}
50 Gauss

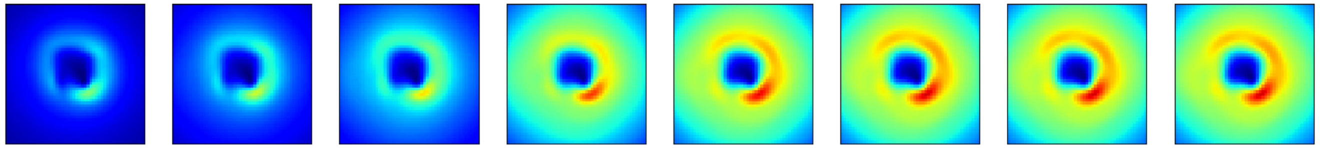

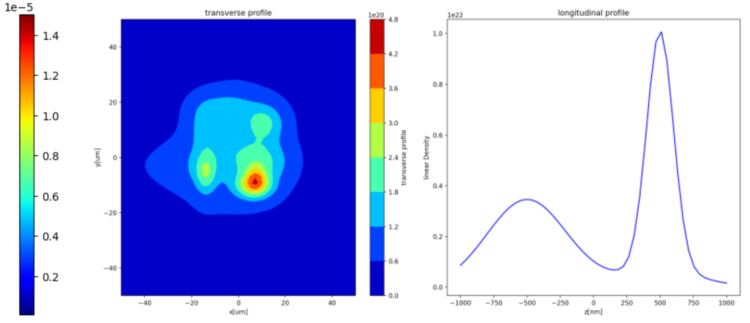

Revealing the $\rho(x_s, y_s, z_s)$ by COTR: Training loss

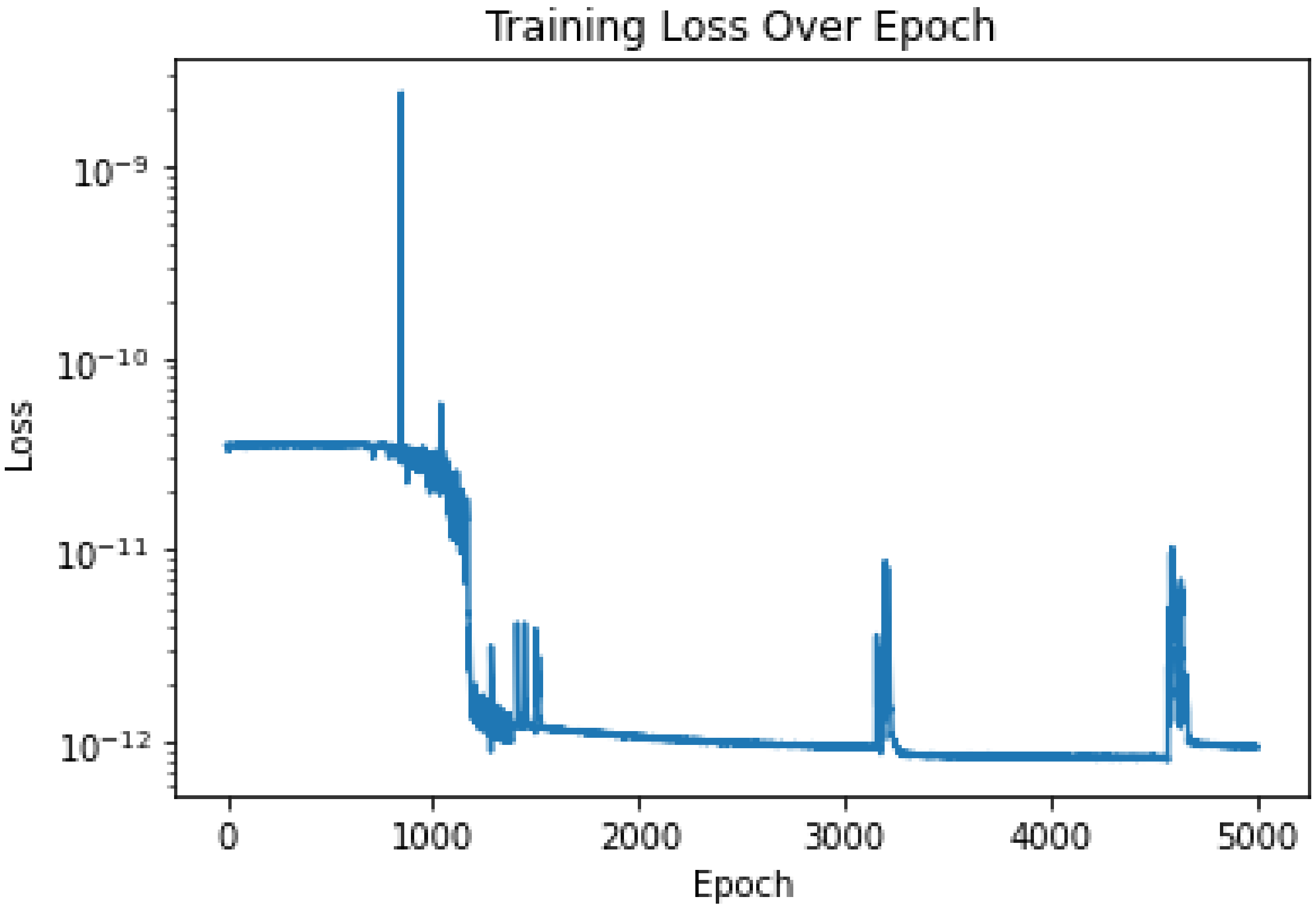

- ~2 hours
- Final loss reduced to 1/50 of the initial loss

Revealing the $\rho(x_s, y_s, z_s)$ by COTR: Neural network "vision"

$\Longrightarrow$

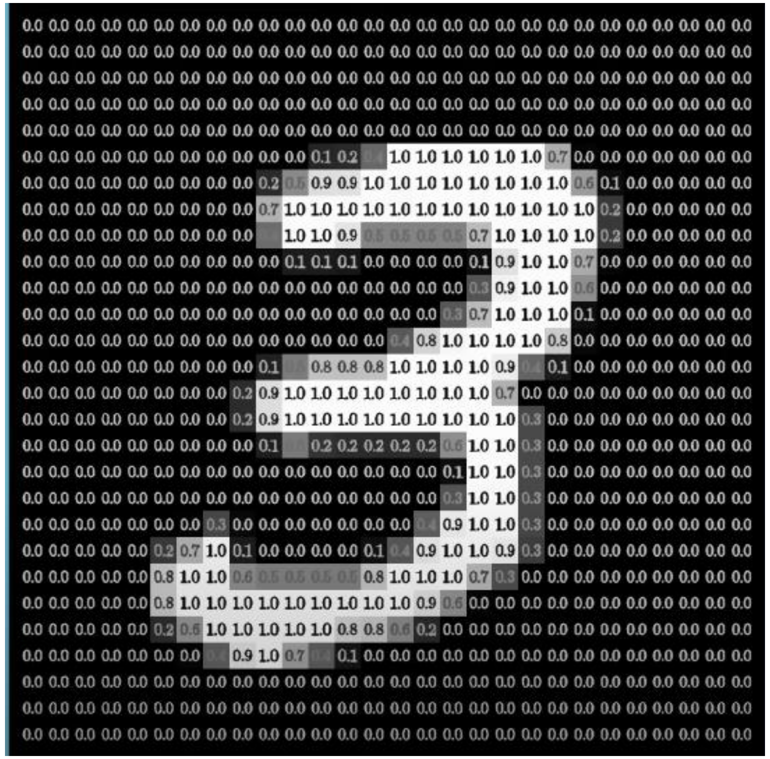

28 by 28

Gray values

$\Longrightarrow$

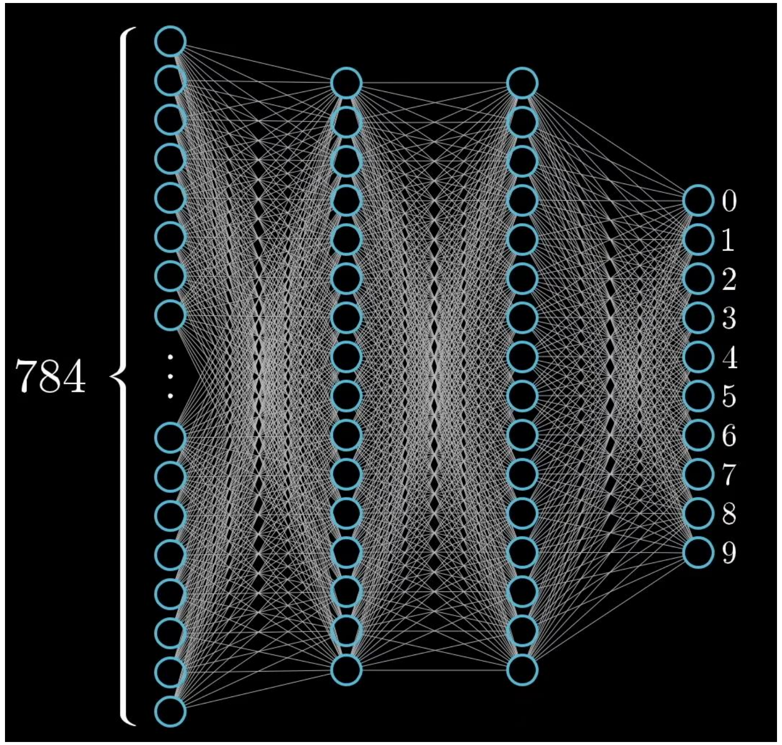

Training repository: paired ρ and S for NN(neural network) to learn

Test repository: paired ρ and S. Given the S, to see if the NN could deduce ρ close to the right one

COTRI Imaging

COTRI is detected in the far field

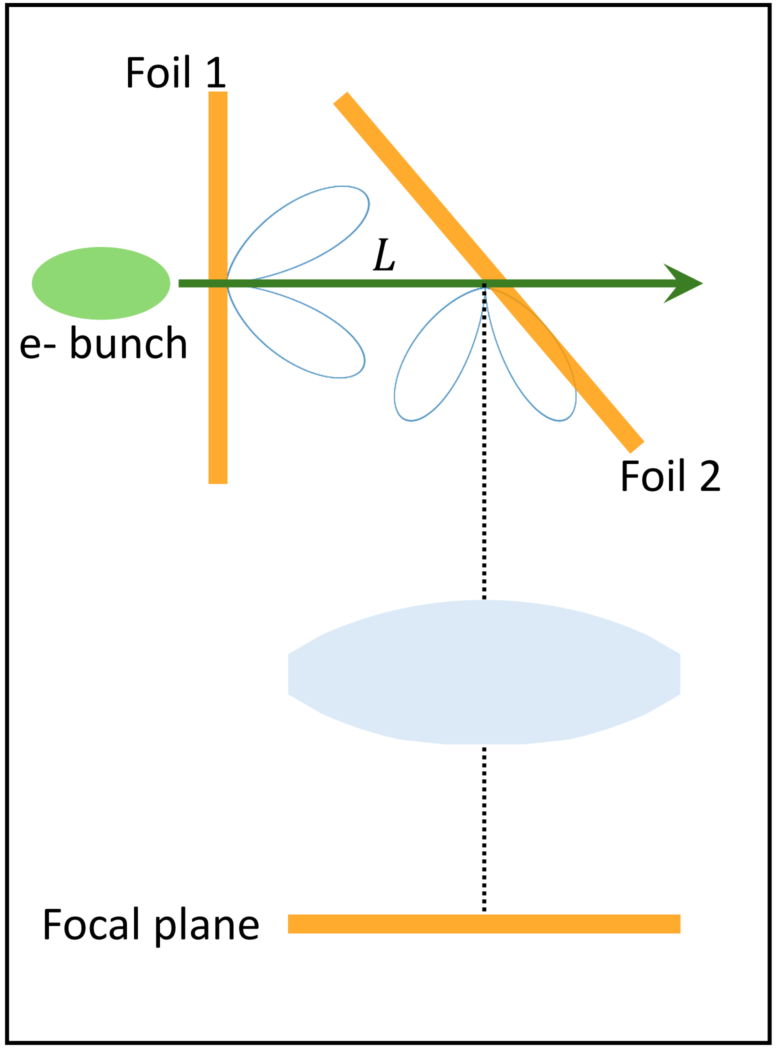

Divergence⇔ Angle of incidence $\boldsymbol{\psi}$ ⟹ Far-field Interferometry

Field point spread function[1]: $E = \frac{e}{\pi\sqrt{c}} \frac{\boldsymbol{\psi}-\boldsymbol{\theta}}{\gamma^{-2}+|\boldsymbol{\psi}-\boldsymbol{\theta}|^2}$

Total E field: $E_{\text{tot}} = E * \underline{h(\boldsymbol{r},\boldsymbol{p})}e^{i\boldsymbol{kr}}$

6D phase space distribution

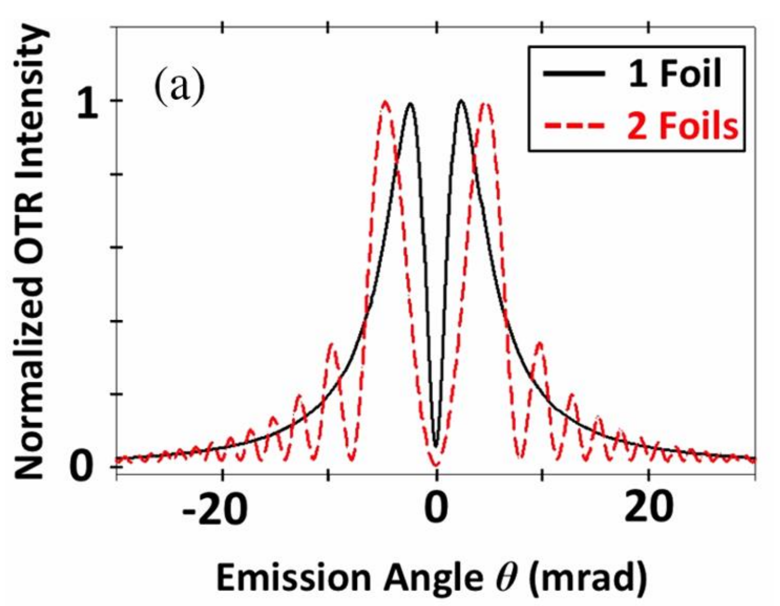

Lumpkin et al, *PRL* **125**, 014801 (2020)

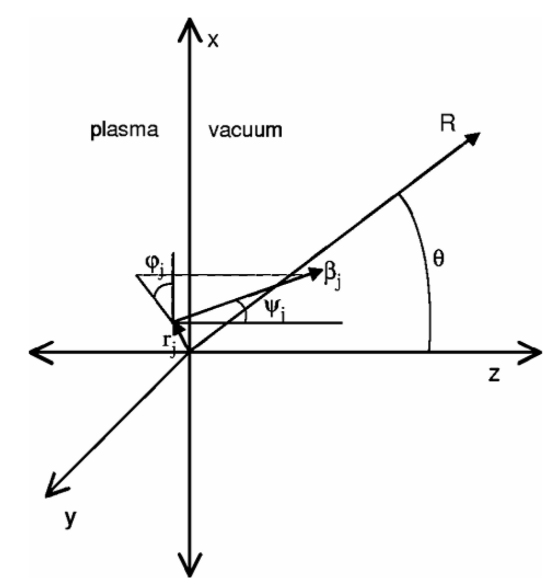

Phys. Rev. E **69**, 016501 (2004)

Fringes contain info of …

1 LaBerge, UT PhD thesis (2022)

Revealing divergence by COTRI

Fringes are sensitive to:

- Optical detection bandwidth $\Delta\lambda$
- Energy bandwidth $\Delta\gamma$
- Transverse size σ_r
- Divergence σ_θ

By choosing $\Delta\lambda$, $\Delta\gamma$, and L $\longrightarrow$ Transverse divergence could be revealed!

σ_r and σ_θ can be dominant

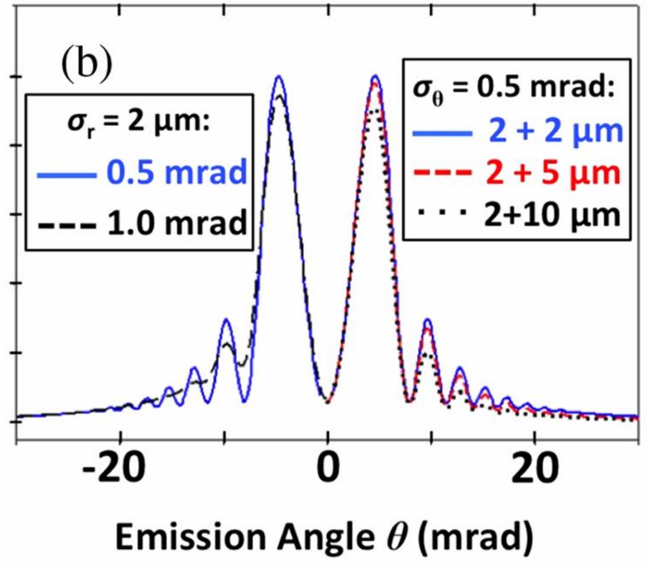

Lumpkin et al, *PRL* **125**, 014801 (2020)

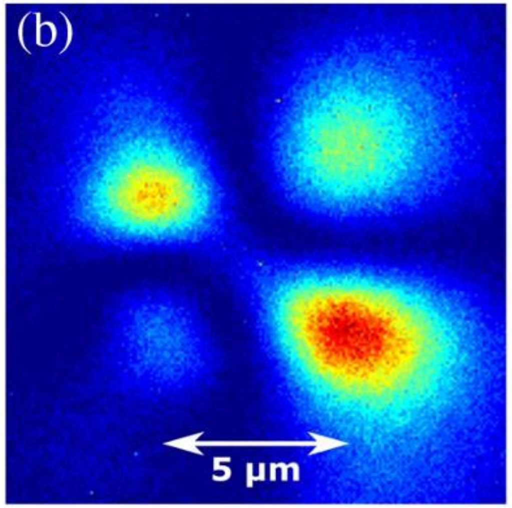

Near-field image

Lumpkin et al, *PRL* **125**, 014801 (2020)

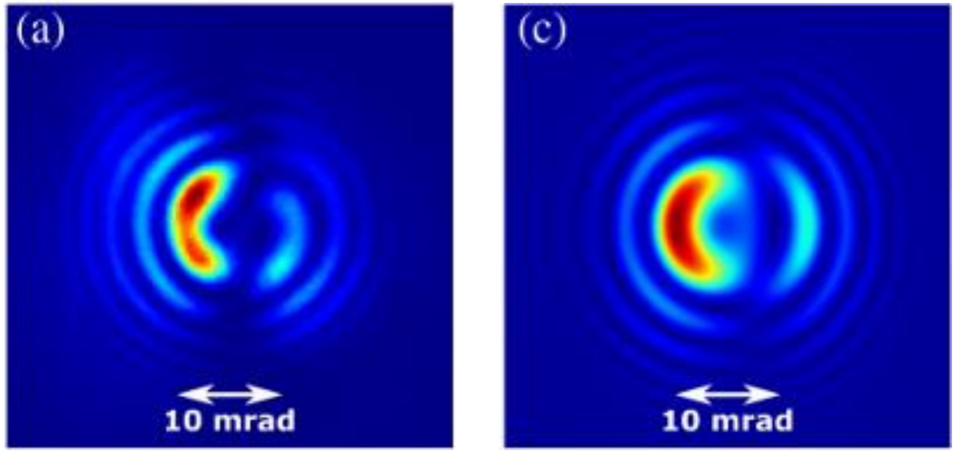

Measured

Reconstructed (σ_θ ≈0.33 mrad)

Lumpkin et al, *PRL* **125**, 014801 (2020)

Quasi-6D structures explored by COTR(I)

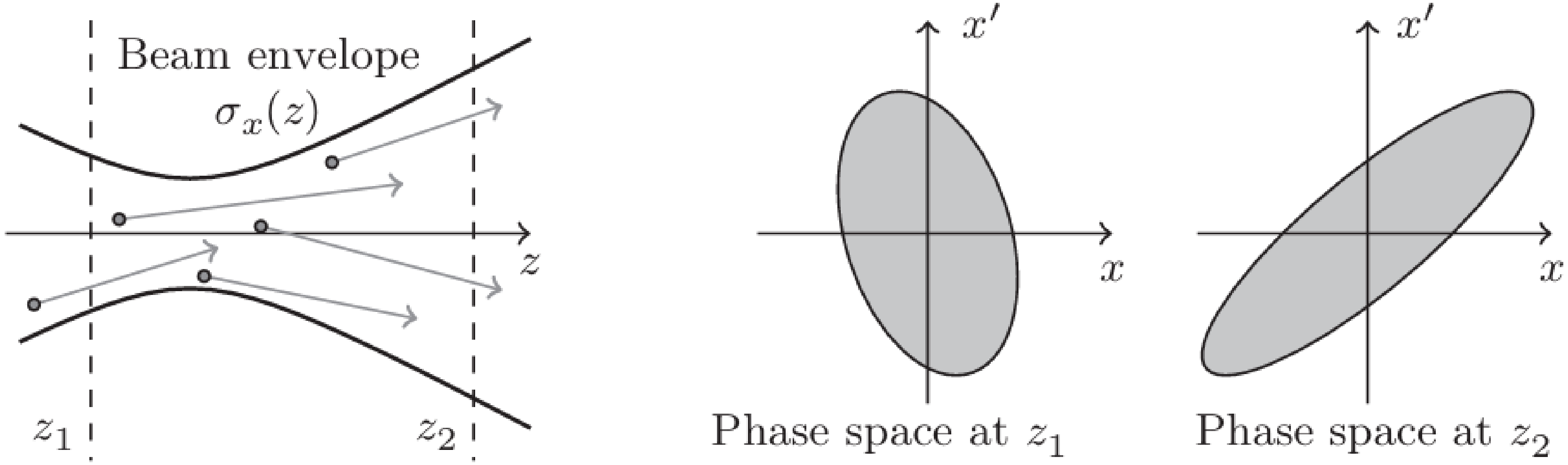

Kim et al, "Synchrotron radiation and free electron lasers", Cambridge University Press (2017)

So far, we have obtained the 5D structures:

- 3D density profile (by COTR)
- 2D transverse divergence (by COTRI)

With reasonable physical assumptions, some phase spaces can be ruled out[1]

→

eg: microbunched portion have lower divergence

Obtain an **upper limit** on transverse emittance on each slice (quasi-1D)

1 LaBerge, AAC 2024

Outline

1. Introduction to LWFA and its diagnostics
2. COTR(I) and quasi-6D structure of e- bunches
3. Future directions, experimental work & conclusion
   - Measurement of form factor
   - Extension to Smith-Purcell Radiation
   - Monitoring the microbunched e- in Free Electron Lasers
   - Combination with Diffraction Radiation

Measurement of form factor

$$\frac{\mathrm{d}^2 W_N}{\mathrm{d}\omega \mathrm{d}\Omega} = [N + N(N-1) \cdot |F(\omega,\theta)|^2] \cdot \frac{\mathrm{d}^2 W_1}{\mathrm{d}\omega \mathrm{d}\Omega}$$

$$F(\omega,\theta) = \int \rho(\boldsymbol{r}) e^{i\boldsymbol{kr}} \mathrm{d}\boldsymbol{r} \quad \text{(Form factor)}$$

With longitudinal and transverse profile separatable:

$$F(\omega,\theta) = F_\perp(\omega,\theta) F_{\boldsymbol{z}}(\omega,\theta) = \int \rho_\perp(\boldsymbol{r}_\perp) e^{i\boldsymbol{k}_\perp \boldsymbol{r}_\perp} \mathrm{d}\boldsymbol{r}_\perp \int \rho_z(z) e^{ik_z z} \mathrm{d}z$$

Suppose the e- bunch takes a bi-Gaussian shape:

$$\rho(\boldsymbol{r}) = \rho_\perp(\boldsymbol{r}_\perp)\rho_z(z) = \frac{1}{\sqrt{2\pi}^3 \sigma_\perp^2 \sigma_z} e^{-\frac{r_\perp^2}{2\sigma_\perp}} e^{-\frac{z^2}{2\sigma_z}}$$

We have $|F_\perp(\omega,\theta)| = e^{-2\pi^2 \frac{\sigma_\perp^2}{\lambda^2} \sin^2\theta}$ (close to unity if $\sigma_\perp \ll \gamma\lambda$)[1]

$$|F_z(\omega,\theta)| = e^{-2\pi^2 \frac{\sigma_z^2}{\lambda^2} \cos^2\theta}$$

$$|F(\omega,\theta)| \approx |F_z(\omega,\theta)|$$

With inverse Fourier transform:

$$\rho_z(z) = \frac{1}{2\pi} \int F(\omega,\theta) e^{\frac{i\omega z}{c}} \mathrm{d}\omega$$

- **With the knowledge of form factor, we can reconstruct the longitudinal profile of the e- beam.**
- The only general method to go down to sub-fs resolution

1 Potylitsyn et al, “Diffraction Radiation from Relativistic Particles” (2010)

Measurement of form factor: complex value

$F(\omega,\theta)$ is a complex value: $\rho_z(z) = \frac{1}{2\pi}\int F(\omega,\theta)e^{\frac{i\omega z}{c}}\mathrm{d}\omega$

Measurement of the absolute value[1,2]

$$|F(\omega,\theta)| = \frac{\frac{\mathrm{d}W_N}{\mathrm{d}\omega}\cdot\frac{\mathrm{d}W_1}{\mathrm{d}\omega} - N\frac{\mathrm{d}W_1}{\mathrm{d}\omega}}{N(N-1)}$$

1. Interpolation & extrapolation
2. Phase retrieval algorithm
3. Physical constraints

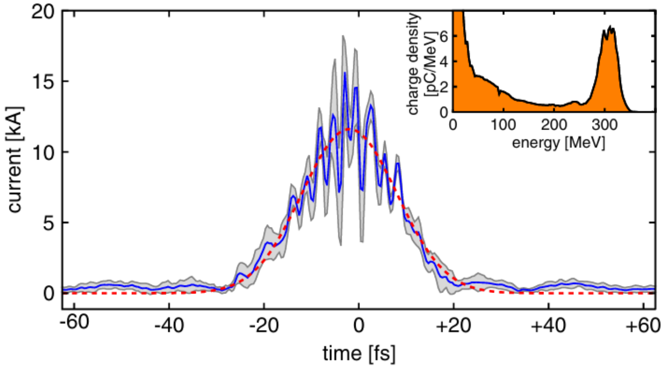

PRAB. **25**, 012801 (2022)

Measurement of the phase:

The phase is closely related to the phase of E field

$$\boldsymbol{E}_{\mathbf{tot}}(\omega,\theta) = \int \mathrm{FPSF}\,(\omega,\theta)\rho_z(z)e^{i\frac{i\omega z}{c}\cos\theta}\mathrm{d}z$$

$|\boldsymbol{E}_{\mathbf{tot}}(\omega)|$ is captured by the camera, phase $\varphi(\omega)$?

To build **phase-sensitive** detectors!

1 Lai et al, *Phys. Rev. E* **50**, 5 (1994)
2 Lai et al, *Phys. Rev. E* **50**, 6 (1994)

Measurement of form factor: spectral interferometry

Self-referenced spectral interferometry[1]

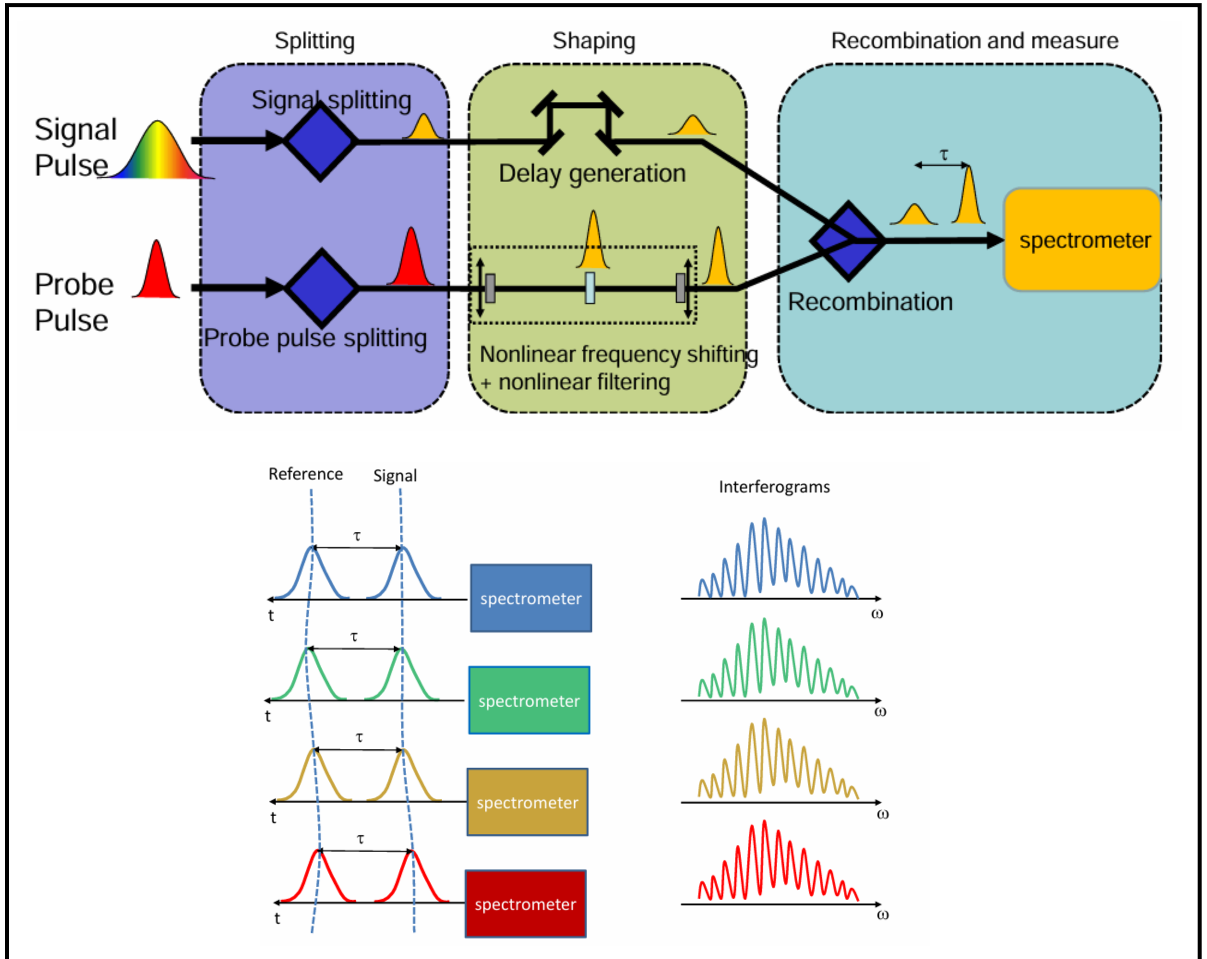

Courtesy of Thomas Oksenhendler

$\tilde{E}_{\text{ref}}$ is well characterized in amplitude and phase[2]

How to detect $\tilde{E}_{\text{sig}}$? From Interferometry

$$\tilde{S}(\omega) = \left|\tilde{E}_{\text{ref}} + \tilde{E}_{\text{sig}}\right|^2 = \tilde{S}_0(\omega) + \tilde{f}(\omega)e^{i\omega\tau} + \tilde{f}^*(\omega)e^{-i\omega\tau}$$

$$\tilde{S}_0(\omega) = \left|\tilde{E}_{\text{ref}}\right|^2 + \left|\tilde{E}_{\text{sig}}\right|^2 \text{ (DC term)}$$

$$\tilde{f}(\omega) = \tilde{E}_{\text{ref}}\tilde{E}^*{}_{\text{sig}} \quad \text{(AC term)}$$

$$\left|\tilde{E}_{\text{ref}}(\omega)\right| = \frac{1}{2}\left(\sqrt{\tilde{S}_0(\omega) + 2\left|\tilde{f}(\omega)\right|} + \sqrt{\tilde{S}_0(\omega) - 2\left|\tilde{f}(\omega)\right|}\right)$$

$$\left|\tilde{E}_{\text{sig}}(\omega)\right| = \frac{1}{2}\left(\sqrt{\tilde{S}_0(\omega) + 2\left|\tilde{f}(\omega)\right|} - \sqrt{\tilde{S}_0(\omega) - 2\left|\tilde{f}(\omega)\right|}\right)$$

$$\varphi_{\text{sig}}(\omega) = \varphi_{\text{ref}}(\omega) - \arg\left(\tilde{f}(\omega)\right)$$

1 Oksenhendler et al, *Appl. Phys. B* **99**, 7-12 (2001)

2 Pariente et al, *Nat. Photon.* **10**, 547-553 (2016)

Extension to Smith-Purcell radiation

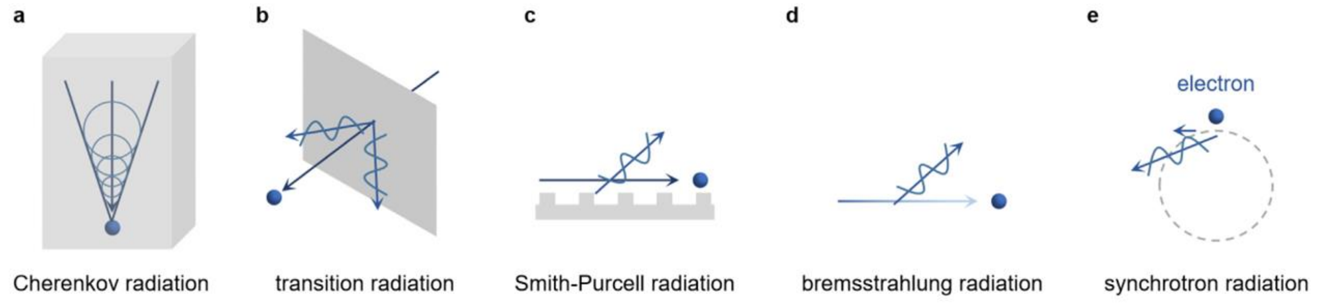

Chen et al, *Mater. Today Electron.* 3 (2023) 100025

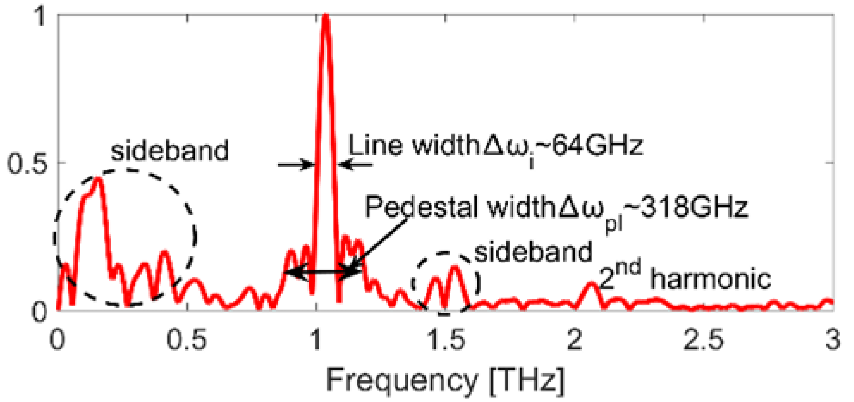

Liang et al, *App. Phys. Lett.* 112, 0253501 (2018)

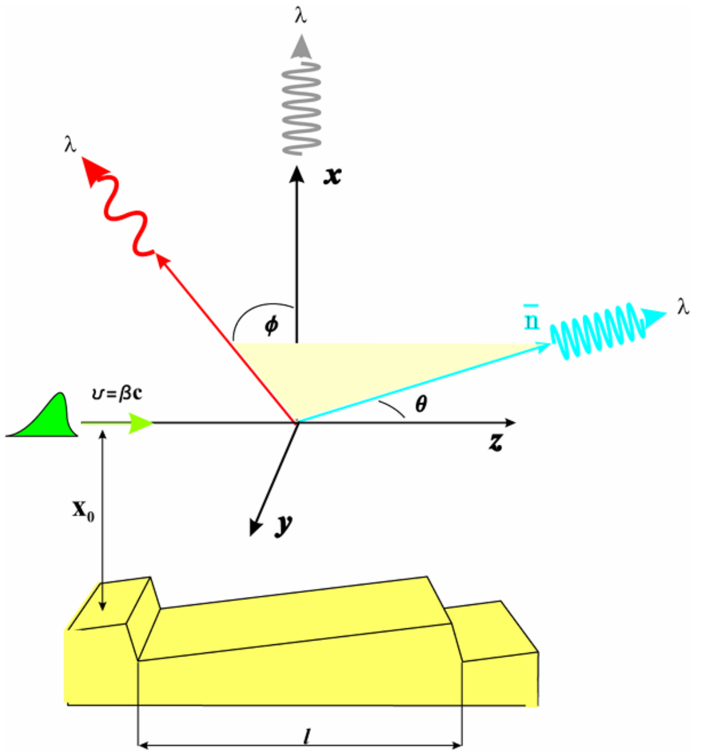

Blackmore et al, *PRST-AB* **12**, 032803 (2009)

SPR angle-wavelength condition

$$\lambda = \frac{l}{n}\left(\frac{1}{\beta} - \cos\theta\right)$$

$$\frac{dW_1}{d\Omega} = 2\pi e^2 \frac{Z}{l} \frac{n^2\beta^3}{(1-\beta\cos\theta)^3} e^{-\frac{2x_0}{\lambda_e}} R^2$$

Coherent emission $\frac{dW_N}{d\Omega} \cong \frac{dW_1}{d\Omega} N^2 S_{\mathrm{coh}}$

where $S_{\mathrm{coh}} = \left| \int T e^{-i\omega t}\, \mathrm{d}t \right|^2$

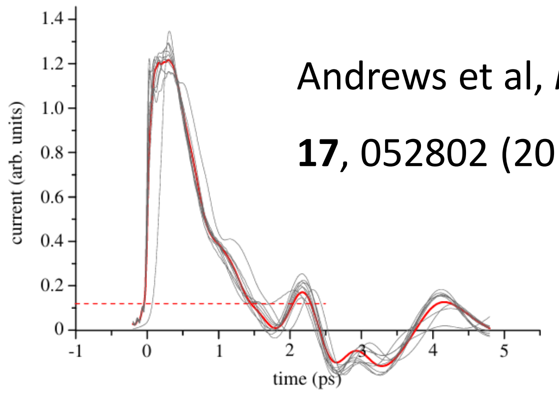

Andrews et al, *PRST-AB* **17**, 052802 (2014)

1. Another source of THz radiation
2. Possesses microbunching info
3. Help to reveal the temporal profile (cross-calibration with COTR)

Monitoring the microbunching in Free Electron Lasers

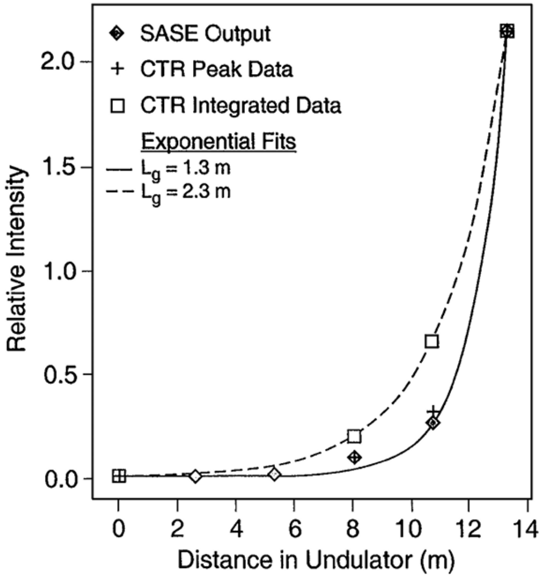

PRL **86**, 79 (2001)

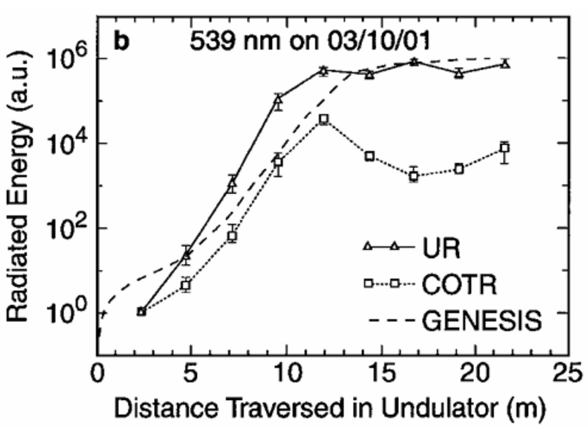

PRL **88,** 234801 (2002)

Seed laser or noise radiation interacting with electrons[1]

⇓

Radiation amplified linearly & e- microbunching growth

⇓

Exponential gain regime & microbunched e-

- **Monitoring the pre-microbunching**

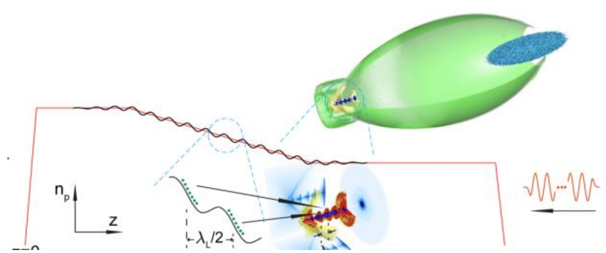

Xu et al, *Nat. Commun.* 13:3364 (2022)

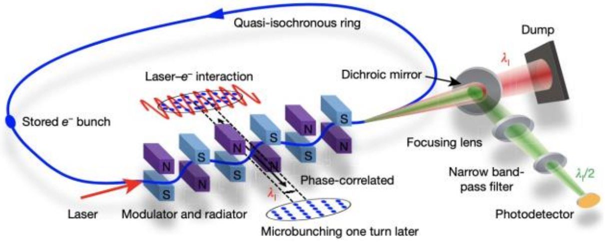

Deng et al. *Nature* **590**, 7847 (2021)

- **Monitoring the microbunching in FEL**

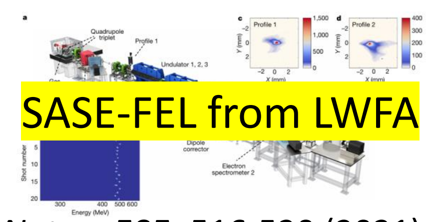

SASE-FEL from LWFA

Nature **595**, 516-520 (2021)

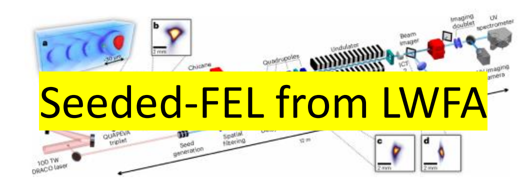

Seeded-FEL from LWFA

Nat. Photon. **17**, 150-156 (2022)

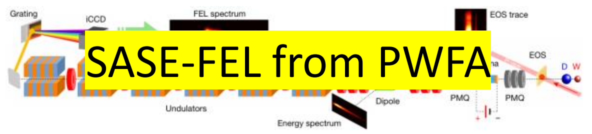

SASE-FEL from PWFA

Nature **605**, 659-662 (2022)

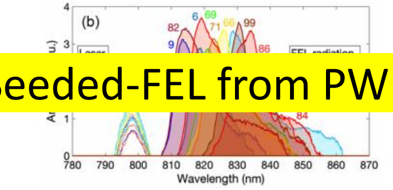

Seeded-FEL from PWFA

PRL **129**, 234801 (2022)

Invasive?

1 *Nat. Photon.* **18**, 780-791 (2024)

Combined with diffraction radiation (DR)[1]

Single-shot & **Non-invasive** diagnostics

Babinet's principle[2]:

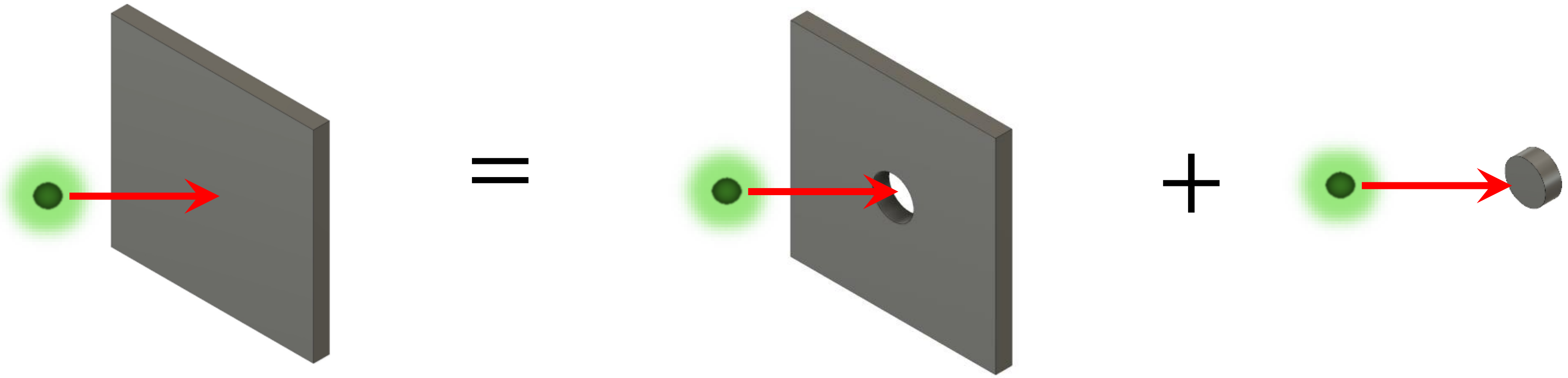

TR from infinite target

DR from hole

TR from finite target

TR from a finite screen can be analytically calculated

$$E_{x,y}^{li}(x_s, y_s, \omega) = -\frac{ie^{ika}}{\lambda a} e^{ik\frac{x_l^2+y_l^2}{2a}} \int \mathrm{d}x_s \mathrm{d}y_s \, E_{x,y}^{s} e^{-ik\frac{x_l x_s + y_l y_s}{2a}} e^{ik\frac{x_s^2+y_s^2}{2a}}$$

1 Potylitsyn et al. *Diffraction Radiation from Relativistic Particles,* Springer (2010)

2 Fiorito et al, *Proceedings of BIW08*, 316-322 (2008)

Upcoming Experimental Work & Conclusion

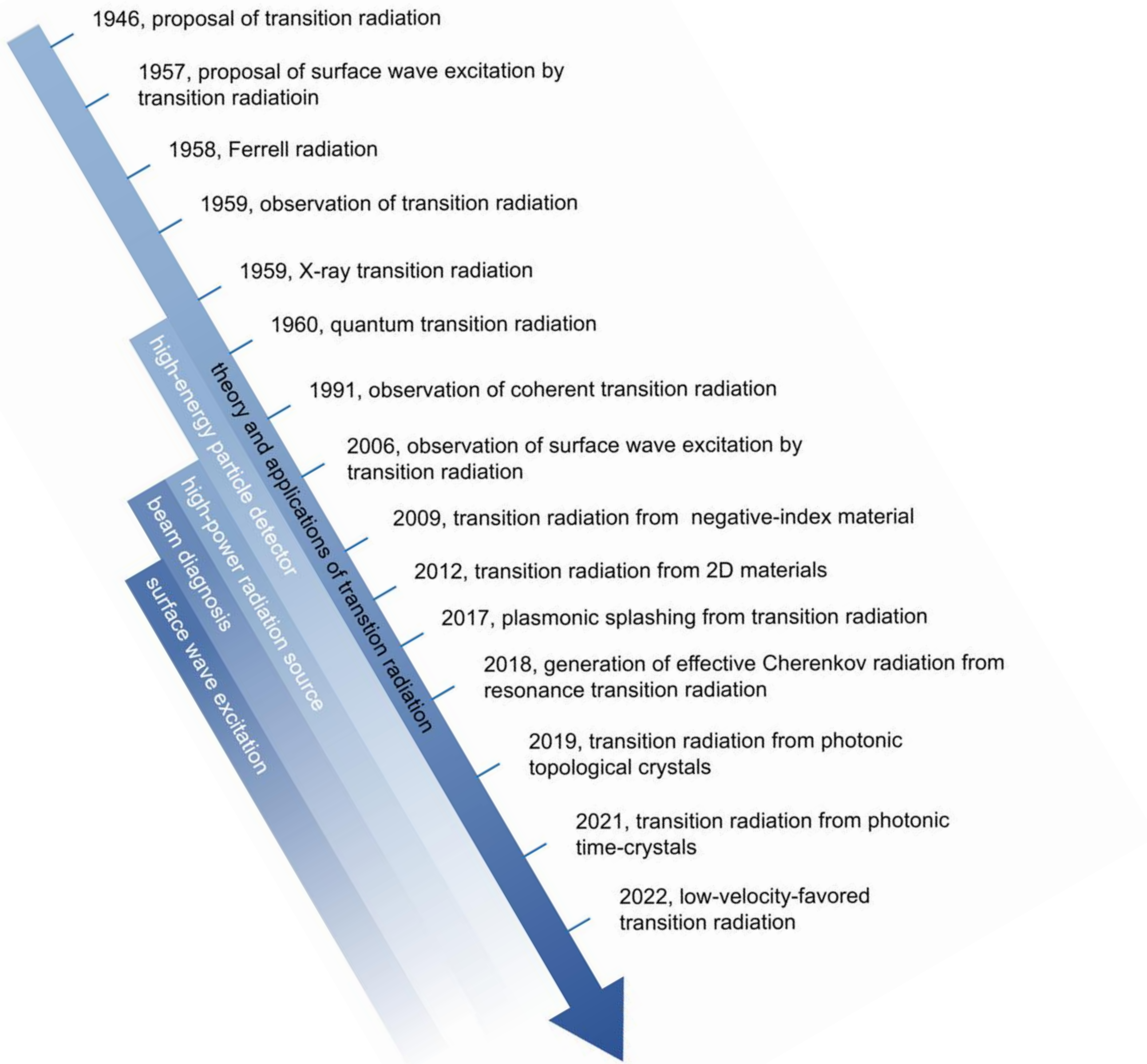

Chen et al, *Mater. Today Electron.* 3 (2023) 100025

Future experimental COTR(I) work is scheduled in UT^3 lab.

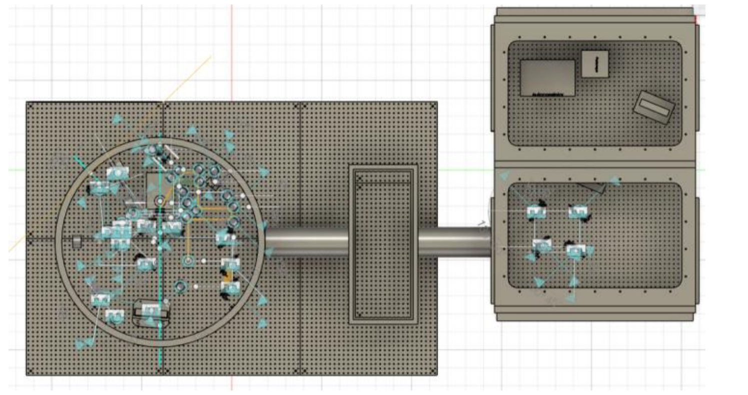

Courtesy of Jason Brooks

Conclusion

1. Introduction on LWFA, and COTR-related diagnostics⇒quasi-6D structure
2. Several possible directions in the future

Thanks

UT-LWFA Group Members:

- Michael Downer (PI)
- Rafal Zgadzaj (Research Scientist)
- Jason Brooks
- Jose Franco Altamirano
- Ross Rudzinsky
- Timothy Araujo
- Yuxuan Cao
- Isabella Pagano
- Dominik Stec
- Bryan Dinh
- Leslie Zhang
- Xiantao Cheng
- Maxwell LaBerge

Courtesy of Google image & Ross